HHS Public Access

Author manuscript

*Neuron*. Author manuscript; available in PMC 2018 August 02.

Published in final edited form as:

*Neuron*. 2017 August 02; 95(3): 623–638.e4. doi:10.1016/j.neuron.2017.06.034.

# Serotonergic modulation enables pathway-specific plasticity in a developing sensory circuit in *Drosophila*

**Takuya Kaneko**[1,*], **Ann Marie Macara**[1,2,*], **Ruonan Li**[1], **Yujia Hu**[1], **Kenichi Iwasaki**[1], **Zane Dunnings**[1], **Ethan Firestone**[1], **Shawn Horvatic**[3], **Ananya Guntur**[4], **Orie T. Shafer**[2], **Chung-Hui Yang**[4], **Jie Zhou**[3], and **Bing Ye**[1,5]

[1]Life Sciences Institute and Department of Cell and Developmental Biology, University of Michigan, Ann Arbor, MI 48109, USA

[2]Department of Molecular, Cellular and Developmental Biology, University of Michigan, Ann Arbor, MI 48109, USA

[3]Department of Computer Science, Northern Illinois University, DeKalb, IL 60115, USA

[4]Department of Neurobiology, Duke University Medical School, Durham, NC 27710, USA

## SUMMARY

How experiences during development cause long-lasting changes in sensory circuits and affect behavior in mature animals is poorly understood. Here we establish a novel system for mechanistic analysis of the plasticity of developing neural circuits by showing that sensory experience during development alters nociceptive behavior and circuit physiology in *Drosophila* larvae. Despite the convergence of nociceptive and mechanosensory inputs on common second-order neurons (SONs), developmental noxious input modifies transmission from nociceptors to their SONs but not from mechanosensors to the same SONs, which suggests striking sensory-pathway specificity. These SONs activate serotonergic neurons to inhibit nociceptor-to-SON transmission; stimulation of nociceptors during development sensitizes nociceptor presynapses to this feedback inhibition. Our results demonstrate that unlike associative learning, which involves inputs from two sensory pathways, sensory-pathway-specific plasticity in the *Drosophila* nociceptive circuit is in part established through feedback modulation. This study elucidates a novel mechanism that enables pathway-specific plasticity in sensory systems.

**Correspondence:** Correspondence and requests for materials should be addressed to B.Y. (bingye@umich.edu).
[5]Lead Contact
[*]These authors contributed equally.



**AUTHOR CONTRIBUTIONS:**

T.K., A.M.M., and B.Y. conceived the project and designed the experiments. T.K., A.M.M, R.L., Y.H., K.I., and Z.D. performed behavior analyses. A.M.M. set up the live-imaging system for the larval nervous system. A.M.M., T.K., and R.L. performed the calcium and cAMP imaging. O.T.S. provided reagents and expertise in stimulating neurons with $P2X_2$ and cAMP imaging. Y.H., K.I., and T.K. carried out the studies on neuronal morphology and connectivity. E.F. and Z.D. set up the optogenetic system for studying larval nociceptive behavior. S.H. and J.Z. developed the method and software for quantifying body angles in larval nociceptive curling. R.L. and A.M.M developed the assay for AITC-induced nociceptive behavior. A.G. and C.Y. provided initial data suggesting that serotonergic neurons are downstream of the nociceptors. B.Y. supervised the project. T.K., A.M.M., and B.Y. wrote the paper.

**Keywords**

*Drosophila*; development; neural circuit; plasticity; pathway-specific; nociceptive behavior; nociceptive circuit; sensory system; serotonin

## INTRODUCTION

The genome directs the wiring of neural circuits so that animals can deal with experiences common to their species. Yet to cope with the uncertainties an individual animal encounters, the nervous system must possess the capacity to modify its circuitry based on that particular animal's sensory experiences. This can be achieved in both mature and developing animals. In fact, sensory experience during development often has a unique and profound impact on the behaviors of mature animals (Hubel and Wiesel, 1970). However, the mechanisms that underlie the experience-dependent plasticity of neural circuits during development are poorly understood.

Sensory-pathway-specific plasticity enables the nervous system to establish long-lasting functional changes in a select modality while maintaining the normal functions of other sensory modalities. Previous studies have discovered such long-lasting, sensory-pathway-specific plasticity in vertebrates. For example, the homeostatic synaptic plasticity in multisensory neurons that receive both visual and mechanosensory inputs in the optic tectum of *Xenopus* tadpoles occurs in a sensory-pathway-specific manner (Deeg and Aizenman, 2011). Very little is known about the mechanisms that mediate sensory-pathway-specific plasticity of neural circuits.

Due to its relatively simple nervous system and amenability to circuit manipulation and genetic analysis, *Drosophila melanogaster* is potentially a good model for revealing the principles of experience-dependent plasticity during development. Studies on the neuromuscular junctions of *Drosophila* larvae have yielded critical insights into mechanisms that underlie activity-dependent plasticity during development (Griffith and Budnik, 2006; Menon et al., 2013; Ruiz-Canada and Budnik, 2006). However, additional experimental systems are needed to elucidate the plasticity mechanisms in the central nervous system (CNS)—which involve interneurons and exhibit convergence and divergence in information flow—and the impact of developmental plasticity on animal behavior. In the larval visual system, prolonged light exposure results in shortened dendrites and reduced calcium responses in neurons postsynaptic to photoreceptors, whereas reduced exposure results in the opposite structural and functional modifications (Yuan et al., 2011). However, how these structural and physiological changes affect larval behavior and whether this system can be used to study interactions among different sensory modalities are unknown. This knowledge gap has motivated us to develop a system that links synaptic physiology to behavior in *Drosophila* to examine the mechanism of sensory-input-induced plasticity during development.

*Drosophila melanogaster* live in a wide range of geographic locations and diverse environments (Singh et al., 1982). During development *Drosophila* larvae encounter noxious stimuli, such as chemicals from plants and pesticides, intense radiation and heat, and harsh

mechanical stimuli from predators. We reasoned that, as *Drosophila* larvae typically live in inescapable environments that contain their food source, adjustment of their nociceptive responses to the surrounding environment would allow them to adapt to the environment for survival and to respond appropriately to true noxious stimuli. In larvae, noxious cues are detected by the nociceptors—called class IV dendritic arborization (C4da) neurons (Figure S1A)—and elicit a series of stereotypical behavioral responses in 3rd instar larvae (Hwang et al., 2007). The same responses can also be induced by direct activation of the nociceptors with channelrhodopsin (ChR2) (Honjo et al., 2012; Hwang et al., 2007). While the morphology and functions of C4da neurons have been well characterized (Corty et al., 2009; Hwang et al., 2007; Kim et al., 2013; Wang et al., 2013; Yang et al., 2014), downstream neurons of the larval nociceptive circuit have just begun to be identified. An elegant study recently demonstrated that C4da nociceptors directly synapse on a group of neurons, termed Basin-2 and −4 neurons, which also receive inputs from mechanosensory neurons and are involved in the multimodal integration of nociceptive and mechanosensory information (Ohyama et al., 2015). Because of this advance, we are now able to analyze the development and physiology of the nociceptive circuit.

In this study, we demonstrate that a feedback circuit motif provides the basis for sensory-pathway-specific plasticity in the developing *Drosophila* nociceptive circuit. We first show that functional development of the nociceptive circuit in *Drosophila* is regulated by noxious sensory inputs. In investigating the underlying mechanism, we identified a group of second-order neurons (SONs) that receive inputs from nociceptors—but not mechanosensors—which reveals that the larval nociceptive circuit contains components for both multimodality integration and modality-specific processing. Taking advantage of this feature of the circuit, we demonstrate that sensory-input-induced plasticity of the nociceptive circuit exhibits a striking degree of pathway-specific adaptation to noxious inputs. We further show that this pathway specificity is, at least in part, achieved through feedback inhibition of the nociceptor presynaptic terminals by serotonergic interneurons. This unique mechanism enables the nervous system to establish long-lasting functional changes in a sensory-pathway-specific manner without disrupting other modalities.

## RESULTS

### Noxious experience during development suppresses larval nociceptive behavior

Stimulation of the nociceptors of *Drosophila* larvae elicits a series of behavioral responses, which begin as an abrupt curling of the body and are often followed by rolling the body along the rostrocaudal axis (Hwang et al., 2007) (Figure 1A). Using the nociceptive circuit and its robust behavioral output as a model, we investigated the functional consequences of exposure to noxious stimuli during development.

Plants have developed various noxious chemical compounds to repel insects. Among these compounds, allyl-isothiocyanate (AITC)—which is found in cruciferous plants and used as a food flavoring, preservative, and, in high concentrations, insecticide (Wu et al., 2009)—acts through TrpA1 channels to excite C4da nociceptors in *Drosophila* larvae (Iwasaki et al., 2008). Consistently, we found that AITC activated C4da neurons (Figure 1B). To test the consequences of exposure to AITC during development, we reared larvae in an environment

containing AITC at a concentration comparable to that found in plants (Sultana et al., 2003). The nociceptive behavioral responses of mature larvae (late 3rd instar) were tested with optogenetic activation of C4da neurons, as described previously (Honjo et al., 2012; Hwang et al., 2007). Larvae raised on AITC exhibited suppression of nociceptive rolling behavior (Figures 1C and S1B), suggesting that noxious stimulation during development suppresses nociceptive behavior.

To determine whether developmental activation of nociceptors is sufficient to suppress nociceptive behavior, we specifically activated C4da neurons during development using an optogenetic approach. ChR2 was specifically expressed in C4da neurons and activated in developing larvae with brief pulses of blue light (5 sec of illumination followed by a 5 min break). Red light, which does not activate ChR2, was used as a negative control. After larval development was complete 5 days after egg laying (AEL), nociceptive behavior was tested with exposure to blue light after at least 1 hr in the dark. Rearing these larvae under pulses of blue light during development dramatically suppressed nociceptive responses, including rolling, curling, and overall response (as demonstrated by changes in body angle) (Figures 1D, S1C, and S1D).

The extent of the sensory-input-induced suppression of nociceptive behavior depended on the intensity of developmental stimulation (Figure 1E). A low intensity of optogenetic stimulation during development led to a behavioral suppression that was comparable to AITC-induced suppression (Figure 1C). Regardless of the intensity, developmental stimulation suppressed the maximal responses (Figure 1E), which effectively reduced the gain of the nociceptive circuit.

ChR2-mediated suppression of nociceptive behavior is not due to the bleaching of all-trans-retinal (ATR), a key component in ChR2 function (Figures S1E and S1F). Consistent with a previous report that intense blue light activates nociceptors (Xiang et al., 2010), illumination with blue light alone (without ATR) during development led to a mild decrease in nociceptive rolling (Figure S1G). Moreover, developmental activation of nociceptors did not change the size or targeting of their presynaptic terminals (Figure S2).

This behavioral suppression was not due to acute changes, because it was absent in larvae reared under constant darkness for 5 days before being illuminated with pulsed red or blue light for 1 hr (Figure 1F). Furthermore, stimulating nociceptors on days 3 and 4 (late 2nd and early 3rd instar larval stages) suppressed the nociceptive response in mature larvae that were tested on day 5 (Figure 1G), suggesting that the functional development of larval nociceptive behavior is regulated by nociceptor activity. This result also demonstrates that the plasticity is long-lasting (> 24 hrs).

Taken together, these results show that noxious experience during development leads to long-lasting suppression of nociceptive behavior in the *Drosophila* larva (Figure 1H).

## A08n neurons are specific postsynaptic targets of nociceptors

To identify the mechanism that underlies the sensory-input-induced plasticity of larval nociceptive behavior, it is necessary to analyze the neurons downstream of the nociceptors.

Recent advances in delineating the larval nociceptive circuit have identified two groups of segmentally repeated neurons, Basin-2 and −4, as postsynaptic targets of both nociceptors and NompC-expressing mechanosensory neurons (Ohyama et al., 2015). In addition, a pair of neurons, called A08n, have been identified as potentially postsynaptic to C4da neurons (Vogelstein et al., 2014) (Figure 2A). Using an improved GRASP technique, termed synaptobrevin-GRASP (syb-GRASP) (Macpherson et al., 2015), we found that A08n dendrites are synaptic partners of C4da axon terminals, but not those of mechanosensory neurons (Figures 2B and 2C), raising the possibility that C4da-to-A08n synaptic transmission is dedicated to the nociceptive circuit. To test this, we used calcium imaging to record nociceptor-evoked responses of A08n and Basin-4 neurons. Activation of nociceptors by AITC elicited robust responses in A08n neurons (Figure 2D). These AITC-elicited responses are nociceptor-dependent, because no response was observed when C4da neurons were genetically ablated or the peripheral nervous system (PNS) disconnected from the CNS. As shown later in Figure 3, the nociceptor-elicited responses in A08n neurons were further confirmed by chemogenetic stimulation of nociceptors. In contrast, activation of mechanosensors did not elicit any response in A08n neurons (Figure 2E), suggesting that C4da-to-A08n transmission is dedicated to the nociceptive circuit. Consistent with the previous report that Basin-4 is postsynaptic to both nociceptors and mechanosensors (Ohyama et al., 2015), Basin-4 responded to activation of both nociceptors and mechanosensors (Figures 2F and 2G).

The role of A08n neurons in larval behavior has not been identified, although optogenetic stimulation of GMR82E12-GAL4-expressing neurons, which includes A08n neurons, leads to a behavior probability distribution that resembles the behavioral output caused by nociceptor activation (Vogelstein et al., 2014). Indeed, optogenetic stimulation of GMR82E12-Gal4-expressing neurons by CsChrimson elicited abrupt body curling (Klapoetke et al., 2014), indicating that these neurons play a major role in the initial step of nociceptive behavior (Figure 2H). In addition to the A08n neurons in the ventral nerve chord (VNC), the GMR82E12-GAL4 driver marks some neurons in the central brain. To confirm the role of A08n neurons in nociceptive behavior, we took advantage of the FLP-out mosaic technique to express CsChrimson in both, one, or none of the two A08n neurons (Gordon and Scott, 2009; Struhl and Basler, 1993; Yang et al., 2014) (Figures 2I and S3). With no expression of CsChrimson in A08n neurons, larvae rarely exhibited nociceptive response despite CsChrimson expression in the central brain. On the other hand, larvae expressing CsChrimson in both A08n neurons exhibited nociceptive behavioral responses at the same level as larvae that expressed CsChrimson in all GMR82E12-GAL4 neurons; larvae expressing CsChrimson in one of the two A08n neurons responded at about half the level of those that expressed in both neurons. Therefore, activating A08n neurons is sufficient to elicit nociceptive behavior. We then silenced the A08n neurons by expressing the inwardly rectifying potassium channel Kir2.1 in these neurons (Baines et al., 2001; Hodge, 2009; Johns et al., 1999) while simultaneously stimulating ChR2-expressing C4da neurons, and recorded behavioral responses. Larvae with inhibited A08n neurons showed a reduction in nociceptive behavior in response to C4da activation (Figure 2J). The incomplete suppression of nociceptive behavior in the absence of A08n activity is likely because the nociceptive circuit consists of multiple pathways downstream of C4da nociceptors, such as the Basin-

Goro pathway (Ohyama et al., 2015). These results demonstrate that A08n neurons mediate nociceptive behavior.

## Nociceptor-input-induced plasticity is sensory-pathway-specific

Results presented so far show that increased input through nociceptors during development leads to long-lasting suppression of nociceptive behavior. Moreover, while Basin-4 neurons receive synaptic inputs from both nociceptors and mechanosensors, A08n neurons receive synaptic inputs from nociceptors but not mechanosensors. Next, we set out to identify where the plasticity occurs. We first examined the activity of the nociceptive-pathway-specific target neurons A08n by calcium imaging. Nociceptors were stimulated during development by either ChR2-mediated optogenetics followed by acute AITC stimulation in mature larvae for calcium imaging (Figures 3A and S4) or by AITC during development followed by acute chemogenetic activation of nociceptors for calcium imaging (Yao et al., 2012) (Figures 3B–3D). In the chemogenetic approach, the vertebrate $P2X_2$ receptor, an ATP-activated cation channel absent in *Drosophila* (Hu et al., 2010; Lima and Miesenbock, 2005), was specifically expressed in nociceptors. Perfusion with solutions containing ATP activates $P2X_2$ (Yao et al., 2012; Zemelman et al., 2002) and, consequently, stimulates nociceptors.

A08n neurons' response to nociceptor stimulation was significantly reduced after developmental stimulation (Figures 3A and 3B). A similar reduction in A08n response was caused by C4da activation on days 3 and 4 of development (Figures S4), which is consistent with the behavioral output (Figure 1G).

We next took advantage of the multimodal inputs to Basin-4 to study the specificity of sensory-input-induced plasticity of the larval nociceptive circuit. After developmental treatment of AITC, Basin-4's responses to nociceptor stimulation were significantly reduced (Figure 3C). In contrast, Basin-4 response to mechanosensor stimulation was not affected by enhanced noxious inputs during development (Figure 3D).

Suppression of C4da-to-SON transmission by developmental stimulation was not caused by changes in sensory transduction in the nociceptors, because no change in calcium response in either C4da somata or their axon terminals was observed (Figures 3E and 3F).

These results suggest that nociceptive inputs during development specifically suppress synaptic transmission from nociceptors to SONs, but not from mechanosensors—even to the same SONs (Figure 3G).

## Serotonergic neurons are required to establish sensory-input-induced plasticity of the larval nociceptive circuit

Next, we set out to determine what mediates developmental experience-dependent suppression of nociceptive behavior. The serotonergic system is involved in synaptic and behavioral plasticity of the mature nervous system in various species, including mammals (Lesch and Waider, 2012), *Aplysia* (Kandel, 2001), and *C. elegans* (Zhang et al., 2005). In *Drosophila* larvae, the processes of serotonergic neurons, which specifically express tryptophan hydroxylase (TRH) (Huser et al., 2012), are near the C4da axon terminals (Figure 4A). This raises the possibility that serotonin (5-HT) modulates synaptic

transmission from C4da neurons to their targets and contributes to the synaptic and behavioral plasticity of the larval nociceptive circuit.

To test this, we silenced serotonergic neurons and examined the consequences for nociceptive behavior. Silencing serotonergic neurons partially rescued nociceptive behavioral responses in larvae whose nociceptors had been stimulated during development (Figures 4B and 4C). Silencing serotonergic neurons did not affect nociceptive behavioral responses when nociceptors were not stimulated during development (Figure S5). These results suggest that serotonergic neurons are required to establish nociceptive-input-induced plasticity in larvae.

We next investigated whether enhancing serotonergic signaling during development leads to suppression of nociceptive behavior. Feeding larvae with the precursor to serotonin, 5-hydroxytryptophan (5-HTP), which increases serotonin levels in the body (Yuan et al., 2006), led to subdued nociceptive behavior (Figure 4D). Feeding 5-HTP, which has a half-life of about 4 hrs (Westenberg et al., 1982), to larvae during the first two days of development also suppressed nociceptive behavior (Figure 4E), suggesting that the effects on behavior are due to developmental changes in the nociceptive circuit.

Consistent with the results from behavioral studies, silencing serotonergic neurons rescued A08n responses to nociceptors in mature larvae that had experienced chronic noxious inputs (Figure 4F), while feeding larvae with 5-HTP led to a suppression of C4da-to-A08n transmission (Figure 4G). Furthermore, optogenetic activation of serotonergic neurons during development reduced C4da-to-A08n transmission (Figure 4H). Since serotonergic neurons were not activated during calcium imaging in these experiments, this result again demonstrates that developmental activation of serotonergic neurons suppresses C4da-to-SON synaptic transmission.

Taken together, these results suggest that serotonergic neurons play an essential role in establishing nociceptive-input-induced plasticity in the developing larval nociceptive circuit.

## Stimulation of nociceptors activates serotonergic neurons via second-order neurons in the nociceptive pathway

To understand how serotonergic neurons contribute to nociceptor-input-induced plasticity, we investigated whether nociceptors regulate the activity of serotonergic neurons. Stimulation of nociceptors activated serotonergic neurons in larval VNC (Figure 5A). Silencing A08n, Basin-4, or all four Basin (Basin-1–4) neurons partially reduced nociceptor-induced activation of serotonergic neurons (Figure 5B), suggesting that nociceptors activate serotonergic neurons through the SONs. To directly test this, we stimulated A08n or Basin-4 neurons with ATP/$P2X_2$ and found that both SONs activated serotonergic neurons (Figure 5C). These results suggest that stimulation of nociceptors activates serotonergic neurons through the SONs.

## Serotonergic signaling inhibits nociceptor-to-SON transmission

We then investigated how serotonergic signaling modulates nociceptor-to-SON synaptic transmission. Our results suggest that serotonergic signaling modulates this synapse through

presynaptic inhibition (Figure 5D). First, ipsapirone, an agonist of the vertebrate 5-HT1a receptor (Glaser and Traber, 1985; Maj et al., 1987; Traber et al., 1984), inhibited C4da-to-A08n transmission (Figures 5D and 5E). In *Drosophila*, ipsapirone may act as an agonist to both 5-HT1a and 5-HT1b, since these two receptors are similarly homologous to mammalian 5-HT1a receptors (Saudou et al., 1992). Second, ipsapirone reduced nociceptor-evoked increases in cyclic AMP (cAMP) levels in C4da presynaptic terminals (Figure 5F). Because 5-HT1 receptors are G-protein-coupled receptors (GPCRs) that down-regulate cAMP levels in cells (Raymond et al., 1999), this result (Grueber et al., 2003; Shafer et al., 2008)suggests serotonergic modulation of C4da presynaptic terminals. Last, RNAi-mediated knockdown of 5-HT1b in C4da neurons, but not those of 5-HT1a or an unrelated protein (mCherry), reduced inhibition of C4da-to-A08n transmission by ipsapirone (Figure 5G). In contrast, knockdown of 5-HT1b in A08n neurons had no effect (Figure 5H). These results suggest that 5-HT1b in C4da axon terminals mediates inhibition of nociceptor-to-A08n transmission by serotonin.

Consistent with physiological results, we found that the terminals of serotonergic neurons intimately intertwined with C4da presynaptic terminals (Figure S6A). However, we did not detect significant syb-GRASP signal from serotonergic terminals to C4da presynaptic terminals (Figure S6B). This suggests that the distance between serotonergic terminals and C4da presynaptic sites are larger than that of conventional synapses (< 100 nm). This finding may not be surprising because serotonergic terminals are known to modulate synaptic transmission through volume transmission or extra-synaptic transmission. In fact, 5-HT1b receptors are found predominantly at extrasynaptic and nonsynaptic sites in rat brains (Riad et al., 2000).

Taken together, these results suggest that SONs activate serotonergic neurons to inhibit nociceptor-to-SON synaptic transmission by acting on nociceptor presynaptic terminals, forming an inhibitory feedback loop (Figure 5I).

## Developmental stimulation of nociceptors sensitizes nociceptor presynaptic terminals to serotonergic inhibition

Our finding of feedback serotonergic modulation led us to hypothesize that developmental stimulation of nociceptors alters the level of this modulation to establish plasticity in C4da-to-SON transmission. Developmental stimulation of C4da neurons did not affect C4da-elicited responses of serotonergic neurons (Figure 6A). Thus, we tested the possibility that developmental stimulation sensitizes nociceptor presynaptic terminals to serotonergic inhibition of C4da-to-SON transmission. Results from two experiments support this possibility. First, 1 μM ipsapirone significantly inhibited C4da-to-A08n transmission after developmental stimulation of nociceptors, but not when nociceptors were not stimulated during development (Figure 6B). Similarly, while 10 μM ipsapirone only partially inhibited C4da-to-A08n transmission when nociceptors were not stimulated during development, it completely inhibited this synaptic transmission after developmental stimulation of nociceptors. These results indicate enhanced sensitivity to ipsapirone of C4da-to-A08n synaptic transmission. Second, developmental stimulation of nociceptors significantly

reduced the sensory-input-induced increase in cAMP levels in C4da axon terminals (Figures 6C and 6D) without affecting basal cAMP levels (Figure 6E).

Consistent with a change in presynaptic modulation of nociceptor-to-target transmission, developmental stimulation of nociceptors did not reduce the responsiveness of SONs. Larval sensory neurons are known to use acetylcholine (ACh) as the transmitter (Salvaterra and Kitamoto, 2001). We tested A08n responses to different concentrations of nicotine, which specifically activates ionotropic AChRs, and recorded A08n response by calcium imaging. Developmental activation of nociceptors did not reduce A08n's response to nicotine (Figure 6F).

Taken together, these results suggest that nociceptor activity during development enhances 5-HT1R–mediated inhibition of nociceptor-to-SON transmission by regulating presynaptic terminals. Such sensory afferent-specific regulation of presynaptic terminals likely maintains the function of other sensory pathways that share central neurons with the nociceptive circuit.

## DISCUSSION

We define here a novel mechanistic model that explains pathway-specific, experience-dependent plasticity during development. Nociceptors activate SONs in the nociceptive circuit, which in turn activate modulatory serotonergic neurons; the latter suppress transmission from nociceptors to SONs, thereby forming a feedback circuit motif. During development, stimulation of nociceptors activates serotonergic neurons to sensitize nociceptor presynaptic terminals to serotonergic inhibition, reducing nociceptive behavioral responses in mature larvae (Figure 6G).

### Sensory gating through presynaptic inhibition at the first synapse of the nociceptive circuit

To prevent an overload of irrelevant or low-priority information, the nervous system filters out sensory afferents elicited by redundant or unnecessary stimuli. Although this process, referred to as "sensory gating", occurs at multiple levels in the nervous system (Freedman et al., 1996; McCormick and Bal, 1994), presynaptic inhibition at the first synapse of sensory pathways appears to be a recurrent theme in sensory gating across species. For example, in the *Drosophila* olfactory system, GABAergic inhibition of the terminals of olfactory receptor neurons (ORNs) controls the information flow in the olfactory circuit (Olsen and Wilson, 2008; Root et al., 2008); the levels of presynaptic inhibition, which are mediated by $GABA_BR2$ receptors, are different in distinct types of ORNs to achieve appropriate responses to various olfactory cues (Root et al., 2008).

Previous studies in other organisms have shown that presynaptic inhibition of nociceptor terminals controls the sensory afferent in the nociceptive pathway. Both external stimuli and internal activities can inhibit nociceptors-to-SON synaptic transmission and, consequently, alter the animal's response to noxious stimuli (Fields, 2004; Kuner, 2010). This allows the animal to ignore noxious stimuli so that it can perform other behavior(s) that may be more

important or—in an inescapable situation—adapt to the stimuli. Whether or not the presynaptic inhibition of nociceptor terminals exists in *Drosophila* was unknown.

In the present study, we discovered presynaptic inhibition at the first synapse of nociceptive circuit in the *Drosophila* larva. Moreover, we found that serotonergic signaling mediates this presynaptic inhibition. Serotoninergic systems are known to modulate sensory gating in several animal species. For example, in the medicinal leech, feeding inhibits the synaptic transmission from tactile mechanosensory neurons to all their SONs (Gaudry and Kristan, 2009), which can be mimicked by serotonin and blocked by an antagonist of serotonin receptors. Such a modulation of sensory gating establishes the priority of feeding over tactile behaviors. Moreover, in *Drosophila*, serotonin modulates olfactory processing by enhancing olfactory responses of the SONs—the projection neurons—in an odorant-specific fashion (Dacks et al., 2009). Therefore, serotonergic inhibition of the first synapse of sensory circuits is a mechanism that underlies sensory gating in multiple sensory systems. Our study shows that serotonergic neurons are part of a feedback loop that inhibits nociceptor-to-SON synaptic transmission in the *Drosophila* larva, which reveals a circuit motif that underlies the presynaptic inhibition of the first synapse of nociceptive circuit (Figure 7).

## A novel mechanism that underlies sensory-pathway specificity in sensory-input-induced plasticity

Our results demonstrate pathway specificity in the plasticity of *Drosophila* nociceptive circuit. Although mechanosensory and nociceptive pathways converge on shared SONs (e.g., Basin-4) to integrate inputs from two different sensory modalities (Ohyama et al., 2015), developmental noxious input only modifies nociceptor-to-SON transmission (Figures 3A–D). A unique aspect of this form of plasticity is that it is mediated through a group of interneurons (i.e., the serotonergic neurons) that receive inputs from SONs (Figure 7). Several aspects of this circuit motif contribute to sensory-pathway-specificity of the plasticity. First, it is different from the serotonergic facilitation that occurs during sensitization of the defensive gill-withdrawal reflex in *Aplysia*, in which serotonergic neurons are activated by another sensory pathway (Kandel, 2001). This makes sense, because the pathway-specific plasticity described here is not a form of associative learning. Co-activation of SONs in the sensory circuit and modulatory interneurons—which provide a feedback control—forms a circuit motif that allows the establishment of long-lasting changes in the nociceptive circuit while maintaining the normal functions of other sensory modalities. Second, the nociceptive circuit establishes plasticity by sensitizing nociceptor presynaptic terminals to serotonin, rather than by enhancing the activity of serotonergic neurons; this allows the nervous system to maintain other serotonin-dependent functions. It is interesting to note that the plasticity achieved through this feedback motif implies a homeostatic mechanism that maintains the activity levels of serotonergic neurons when those of SONs are reduced. Last, by modulating the presynaptic terminals of nociceptors, but not the postsynaptic neurons, nociceptor-input-induced plasticity allows the postsynaptic neurons to maintain their normal responses in other modalities (e.g., mechanosensation) (Figure 3D, G).

### The role of serotoninergic system in the plasticity of sensory gating

We found that the strength of serotonergic modulation is plastic such that stimulation of nociceptors during development sensitizes nociceptor presynaptic terminals to serotonergic inhibition. This plasticity is probably established through use-dependent strengthening of the serotonergic modulation; noxious input during development likely leads to chronic activation of serotonin receptors in nociceptor presynaptic terminals, which in turn sensitizes these presynaptic terminals to serotonergic modulation. The enhanced sensitivity may be achieved through: (a) an increase in the expression level of serotonin receptors in the presynaptic terminals—for example, through CREB-dependent gene expression (Bartsch et al., 1998; Dash et al., 1990); (b) modification of a signaling transduction pathway that leads to reduced presynaptic neurotransmitter release—which would be a novel form of synaptic scaling; or (c) modification of the function of the serotonin transporter in presynaptic terminals (Fabre et al., 2000). Our study lays the foundation for future studies of the molecular pathways that underlie nociceptor-input-induced plasticity.

### Ethological significance of sensory-input-induced plasticity in the nociceptive circuit

Developmental plasticity of the nervous system allows animals to adapt their behaviors to survive in a unique, yet stable, environment. Larvae have fewer degrees of freedom in choosing their environments than do adult flies and other vertebrates. As nociceptive curling and rolling are disruptive to baseline functions of larval nervous system, it is conceivable that developing in an environment in which there is excessive noxious sensory input requires that the animal suppresses nociceptive circuit function for survival. Identification of nociceptive circuit-specific plasticity suggests a neural mechanism for survivability in the presence of noxious environmental factors, such as noxious heat and plant-derived chemicals. This type of behavioral modulation may be useful in the natural environment, as *Drosophila melanogaster* lives in a wide range of geographic locations and environments (Singh et al., 1982). Moreover, some noxious chemicals have antimicrobial properties (Billing and Sherman, 1998; Zhang, 2010) and could potentially protect *Drosophila* from bacteria or deleterious fungi in rotten fruits. Finally, our data show that exposure to low levels of the insecticide AITC results in modulation of insect behavior, which indicates potential unintentional ecological consequences of insecticide off-target effects.

## STAR METHODS

### CONTACT FOR REAGENT AND RESOURCE SHARING

Further information and requests for resources and reagents should be directed to and will be fulfilled by the Lead Contact, Dr. Bing Ye (bingye@umich.edu).

### EXPERIMENTAL MODEL AND SUBJECT DETAILS

***Drosophila Melanogaster* strains—**The following fly stocks are used in this study. Both male and female wandering 3rd-instar larvae are used unless otherwise noted. All experiments will be conducted on age- and size-matched larvae.

GAL4/LexA stocks: GMR82E12-GAL4 (Bloomington *Drosophila* Stock Center, stock number B-40153) and GMR82E12-lexA (B-54417) (Vogelstein et al., 2014); *ppk*-GAL4

(Grueber et al., 2007); *ppk*-LexA (Gou et al., 2014); *nompC*-GAL4 (B-36369); *nompC*-LexA (B-52241); GMR57F07-GAL4 (B-46389), GMR57F07-lexA (B-54899), and GMR72F11-Gal4 (B-39786) (Ohyama et al., 2015); *TRH*-GAL4 (B-38389); *TRH*-LexA (B-52248).

UAS/LexAop stocks: UAS-CD4-GFP (BL-35836); UAS-GCaMP6f (Chen et al., 2013); LexAop-GCaMP6f (Chen et al., 2013) (B-44277); UAS-Epac1-camps (Shafer et al., 2008); UAS-ChR2::YFP (Honjo et al., 2012); UAS-CsChrimson::Venus (B-55139) (Klapoetke et al., 2014); LexAop-P2X$_2$ (Yao et al., 2012); UAS-DenMark (B-33062) (Nicolai et al., 2010); UAS-syt-HA(Robinson et al., 2002); UAS-Kir2.1 (Baines et al., 2001; Nitabach et al., 2002); LexAop-kir2.1 (Prieto-Godino et al., 2012); UAS-syb::spGFP$^{1–10}$(Macpherson et al., 2015) and LexAop-CD4::spGFP$^{11}$ (Macpherson et al., 2015); UAS-RNAi-5-HT1b (B-33418, designated as #1); UAS-RNAi-5-HT1b (B-27635, designated as #2); UAS-RNAi-5-HT1a (B-33885); UAS-RNAi-5-HT7 (B-32471); UAS-FRT-rCD2-stop-FRT-CD8::GFP, UAS-FRT-rCD2-stop-FRT-CD4::tdTomato (Yang et al., 2014).

Other stocks: *hs-flp*$^{122}$ (B-1929), *tub*P-FRT-Gal80-FRT (B-38880), and *ppk*-ChR2::YFP. To make the *ppk*-ChR2::YFP transgenic flies, ChR2-YFP cDNA was amplified from UAS-ChR2::YFP transgenic flies by PCR, cloned into the pBluscript-ENTR-Topo vector, and inserted via Gateway cloning into the pDEST-APPHIH vector between the attR1 and attR2 sites, which are downstream of the 1-Kb promoter of the *ppk* gene. The resulting plasmid, pDEST-APPHIH-ChR2, was then used for transgenesis with the ΦC31 system.

## METHOD DETAILS

**FLP-out mosaic labeling—**Mosaic A08n labeling (Figure 2B) and stimulation (Figures 2I and S3) were achieved by the combination of a FRT-flanked Gal80 transgene that is under the control of a tubulin promoter (*tub*P-FRT-Gal80-FRT), and a transgene expressing heat-inducible flippase (*hs*-FLP) (Gordon and Scott, 2009). Upon flippase-mediated removal of Gal80, A08n neurons express CD4-GFP, DenMark, and Syt-HA (Figure 2B), or CsChrimson::Venus (Figures 2I and S3). UAS-FRT-rCD2-stop-FRT-CD8::GFP and UAS-FRT-rCD2-stop-FRT-CD4::tdTomato (Yang et al., 2014) were used in combination with *hs*-FLP and TRH-GAL4 to label single serotonergic neurons with fluorescent proteins in Figure 4A. Genetic mosaic clones were generated using the method described previously (Yang et al., 2014).

**Behavioral tests—**Embryos were collected for 6–12 hrs at 25 °C on basic fly food. The fly food was mixed with 4 mM ATR for optogenetic stimulation, 2.5 to 5 mM allyl isothiocyanate (AITC, Sigma) for AITC-mediated developmental stimulation, or 5 mM 5-hydroxytryptophan (5-HTP, Sigma) for 5-HTP feeding. On day 5, mature (wandering 3$^{rd}$ instar) larvae were transferred to room temperature, removed from food, rinsed, and left in the dark for 1 hr before being tested for behavioral responses. Control and experimental groups are paired in all behavioral tests.

Optogenetic behavioral tests were done on ø5 mm grape-agar plates covered with 1 ml water in a dark room. For optogenetic stimulations, a light intensity of 26 μW/mm$^2$ was used. 470 nm Blue LED (CREE XP-E Blue 3W LED, RapidLED, Inc.) was used for ChR2 activation.

ChR2-mediated nociceptor stimulation was performed by *ppk*-GAL4/UAS-ChR2::YFP or *ppk*-ChR2::YFP, as indicated in the figures. Neurons in the CNS—A08n and TRH—were stimulated by expressing CsChrimson::Venus using 617 nm red LED (CREE XP-E Red LED, RapidLED, Inc.). LED stimulation was for 5 sec.

AITC behavioral tests were performed on 12-well grape-agar plates. Each well was covered with 300 μl of 25 mM AITC before transferring one larva to the well. Only single larvae were placed on each well so that individual larvae could be tracked for two min.

Sample sizes were estimated based on previous publications in the field (Jovanic et al., 2016; Ohyama et al., 2015). To reduce possible variation in each batch of fly cultures, samples from more than 3 separate trials, each of which included similar numbers of samples, were analyzed. The behavioral tests with AITC as the stimulant were more subject to variations of experimental conditions. To eliminate experimenter bias, these experiments were done in double-blind fashion. The video recorded by the primary experimenter was coded and randomized by another experimenter. After the primary experimenter quantified the data, the recordings were decoded for statistical analysis. All behavioral data were included in the statistical analyses.

**Developmental optogenetic stimulation—**Automatic optogenetic stimulation (26 $\mu W/mm^2$) of nociceptors during development was achieved by a custom-made array of LEDs. Illumination duration and frequency were controlled by a BASIC Stamp microcontroller, and intensity by a PWM Dimmer. LEDs (CREE XP-E Blue 3W LED, CREE XP-E Red LED) were mounted on aluminum heatsinks (RapidLED). For even distribution of light on the agar dish for rearing larvae, the light emitted by LED passes through an 80° CREE XP-E/XP-G lens. Developmental optogenetic stimulation was performed in a 25°C incubator. LEDs were programmed to turn on for 5 sec every 5 min throughout the appropriate experimental duration.

**Calcium and cAMP imaging—**Live imaging of calcium and cAMP levels was conducted on a Leica SP5 confocal microscope equipped with a resonance scanner, an acousto-optical beam splitter, and an HC Fluotar L 25×/0.95 W VISIR immersion objective (Leica). Calcium levels were measured by imaging with the GCaMP6f indicator (Chen et al., 2013). Larvae were dissected as previously described (Matsunaga et al., 2013). Dissection and imaging were performed in a modified hemolymph-like 3 (HL3) saline (70 mM NaCl, 5 mM KCl, 0.5 mM $CaCl_2$, 20 mM $MgCl_2$, 5 mM trehalose, 115 mM sucrose, and 5 mM HEPES, pH 7.2) (Stewart, 1994). 7 mM glutamate was added to the HL3 solution to block muscle contractions and eliminate motor feedback to the sensory circuits by saturating glutamate receptors at the neuromuscular junction (Macleod et al., 2004; Reiff et al., 2005; Reiff et al., 2002). A low concentration of calcium was also used to reduce muscle contraction and nerve damage during dissection (Caldwell et al., 2013). Calcium responses were recorded in xyzt mode such that an image stack was taken every 1 sec or 2 sec over the course of the experiment.

ATP/$P2X_2$ technique was used to stimulate neurons for calcium imaging with the expression of rat ATP-sensitive cation channel $P2X_2$ (Yao et al., 2012). Because there are no ATP-

sensitive channels in *Drosophila*, ATP application excites neurons that express $P2X_2$ (Yao et al., 2012). This approach is particularly instrumental when GCaMP-implemented calcium imaging is used to record neuronal activity due to an overlap in the excitation wavelengths of ChR2, CsChrimson (activated by both red and blue light), and GCaMP. Unless otherwise stated, 1 mM ATP was used to activate neurons expressing $P2X_2$. ATP (Sigma) was first dissolved in water to 100 mM and then diluted to the final concentrations with HL-3. We used the ValveBank®4 Pinch Valve Perfusion System (Automate Scientific) to control perfusion of ATP.

In addition to the ATP/$P2X_2$ technique, AITC was used as a natural stimulant to activate nociceptive neurons, and nicotine to activate A08n neurons. AITC, ipsapirone (Tocris), and (–)-nicotine tartrate (Fisher Scientific) were bath-applied to the specimen; concentrations are indicated in the figure legends. AITC (Sigma) was first dissolved in DMSO to 1 M, and then diluted to the final concentrations with HL-3. In experiments that test the effects of ipsapirone while stimulating nociceptors, ipsapirone was mixed with AITC before being applied to the samples.

cAMP levels were measured by imaging with the Epac1-camps indicator (Shafer et al., 2008; Yao et al., 2012). The procedure for cAMP imaging was the same as that for $Ca^{2+}$ imaging described above except for the following. The Epac1-camps indicator was specifically expressed in nociceptors, whose presynaptic terminals were imaged for Förster resonance energy transfer (FRET). Hence the observed cAMP levels were only those in C4da presynaptic terminals. 2 mM AITC was used to activate nociceptive neurons. In Figure 6C, ipsapirone was mixed with AITC before being applied to the specimen. A Z-stack was taken every 3 sec over the course of the experiment.

Sample sizes were estimated based on previous publications in the field (Jovanic et al., 2016; Ohyama et al., 2015; Yao et al., 2012). To reduce possible variation in each batch of fly cultures, samples from more than 3 separate trials, each of which included similar numbers of samples, were analyzed. Several key findings, including the effects of developmental stimulation on behavior and synaptic transmission and the pathway-specificity of the plasticity were repeated by multiple experimenters. All data were included in the analyses with the exception that neurons with low levels of AITC-evoked responses (<50% Max$\Delta F/F_0$) before ipsapirone treatment were not included in Figure 5G and H. This is to minimize the masking of ipsapirone suppression caused by low levels of initial response.

**Immunostaining—**Third instar larvae were dissected and stained as described previously (Kim et al., 2013; Wang et al., 2013). Primary antibodies used were: mouse anti-GFP (1:100, Sigma, RRID:AB_259941); chicken anti-GFP (1:2500, Aves Laboratories, RRID:AB_2307313); rabbit anti-RFP (1:5000, Rockland, RRID:AB_2209751); and rat anti-HA (1:250, Roche, RRID:AB_390915). Secondary antibodies used were (1:500, Jackson ImmunoResearch): donkey anti-mouse Alexa Fluor 488 (RRID:AB_2340846), anti-chicken Alexa Fluor 488 (RRID:AB_2340375), anti-chicken Alexa Fluor 647 (RRID:AB_2340380), anti-rabbit Rhodamine RX (RRID:AB_2340613), and anti-rat Alexa Fluor 647 (RRID:AB_2340694).

**Synaptobrevin-GRASP—**Syb-GRASP was performed as described previously (Macpherson et al., 2015). Reconstituted GFP (i.e., GRASP) signals were detected by anti-mouse monoclonal GFP antibody (1:100, Sigma, RRID:AB_259941, referred to as anti-GRASP). Syb::spGFP$^{1–10}$ was preferentially detected by anti-chicken polyclonal antibody (1:2500, Aves Laboratories, RRID:AB_2307313, referred to as anti-spGFP$^{1–10}$).

## QUANTIFICATION AND STATISTICAL ANALYSIS

**Quantification of behaviors—**Rolling was counted only when a larva exhibited at least one complete (360°) rotation of the body along a rostrocaudal axis (Hwang et al., 2007). Curling is defined as an acute decrease in body angle formed by simultaneous movements of the head and tail immediately upon noxious stimulation. The numbers of larvae that rolled and curled were manually counted in slow motion (0.5 – 0.25 × speed) over the 5-sec stimulation interval for optogenetic assays or over the 2-min period of AITC stimulation. Percent rolling and curling were the number of larvae that rolled or curled divided by the total number of larvae counted (number of larvae that rolled or curled × 100/Total larvae).

Body angle was calculated as the angle between the two lines that connect the middle point of the skeleton and each of the two end points of the skeleton. The angle ranges between 0 and 180 with a smaller angle indicating a more curled larva. To obtain the skeleton and its middle and end points, a custom ImageJ plugin was developed to first detect and track the larvae at each frame. Contours of the detected larvae were then smoothed using a 3×3 mean filter. A skeletonization algorithm was applied to obtain the centerlines of the detected larvae. A longest-path search was then performed to remove the small spurs and result in a clean centerline of the animal. The middle point of the skeleton is the point on the skeleton line with equal distances to the two end points along the skeleton. The positions of the middle point and two end points of the skeleton line were used for the body angle calculation, as described above.

**Quantification of calcium and cAMP imaging—**The ImageJ software (NIH) with the Time Series Analyzer plugin was used to analyze the xyzt projection movie. The average intensity of a selected region of interest (ROI) was measured over the course of the experiment.

To quantify calcium responses, the change in GCaMP6f fluorescence was calculated by $\Delta F/F0 = (Ft - F0)/F0$, where Ft is the fluorescent mean value of an ROI in a given frame. F0 is the baseline 30-sec interval before stimulation. Max ΔF is the maximum value during the stimulation period of the recording. To analyze the activity levels of A08n neurons, Max ΔF/F0 for individual A08n neurons were plotted on the graph and used for statistical analyses (i.e., each dot indicates one A08n). Because the responses of Basin-4 neurons—unlike A08n neurons—are highly variable within each VNC (data not shown) (Jovanic et al., 2016), the average of Max ΔF/F0 of 10 Basin-4 neurons from abdominal segments 3–7 in each VNC were calculated to represent the Basin-4 activity in each VNC.

The cAMP response level was quantified as changes in the inverse FRET ratio, which is CFP intensity divided by YFP intensity (ΔCFP/YFP) scanned with a 458-nm confocal laser. The cAMP basal level was quantified as YFP intensity scanned with a 458-nm divided by

that scanned with a 515-nm laser ($YFP^{458}/YFP^{515}$). The *n* represents the number of larvae tested.

**Statistical analysis—**Statistical analysis was performed using Prism software. Fractions of rolling and curling behavior under stimulation were analyzed using the chi-squared test. Calcium and cAMP imaging, and axon terminal length of single C4da neurons were analyzed using the Mann-Whitney nonparametric U-test. For multi-group comparisons, Kruskal-Wallis tests were conducted. In all figures, N.S., *, **, and *** represent $p > 0.05$, $p < 0.05$, $p < 0.01$, and $p < 0.001$, respectively. Error bars are standard errors of the mean.

## Supplementary Material

Refer to Web version on PubMed Central for supplementary material.

## Acknowledgments

We thank Marco Gallio and Vivek Jayaraman for generously sharing fly stocks. We also thank Dion Dickman, Songhai Shi, Yang Xiang, Yi Rao, and Kexin Yuan for critical comments on earlier versions of the manuscript. This work was supported by grants from NIH (R21 GM114529-01), Protein Folding Disease Initiative of the University of Michigan, and the Pew Scholars Program in the Biological Sciences to B.Y., an NIH grant (R15MH099569) to J.Z., and an NIH grant (R01GM100027) to C.Y., a Patten Research Scholar Award and a Rackham Predoctoral Fellowship to T.K.. *Drosophila* stocks from the Bloomington *Drosophila* Stock Center (NIH P40OD018537) were used in this study.

## References

Baines RA, Uhler JP, Thompson A, Sweeney ST, Bate M. Altered electrical properties in Drosophila neurons developing without synaptic transmission. J Neurosci. 2001; 21:1523–1531. [PubMed: 11222642]

Bartsch D, Casadio A, Karl KA, Serodio P, Kandel ER. CREB1 encodes a nuclear activator, a repressor, and a cytoplasmic modulator that form a regulatory unit critical for long-term facilitation. Cell. 1998; 95:211–223. [PubMed: 9790528]

Billing J, Sherman PW. Antimicrobial functions of spices: why some like it hot. The Quarterly review of biology. 1998; 73:3–49. [PubMed: 9586227]

Caldwell L, Harries P, Sydlik S, Schwiening CJ. Presynaptic pH and vesicle fusion in Drosophila larvae neurones. Synapse. 2013; 67:729–740. [PubMed: 23649934]

Chen TW, Wardill TJ, Sun Y, Pulver SR, Renninger SL, Baohan A, Schreiter ER, Kerr RA, Orger MB, Jayaraman V, et al. Ultrasensitive fluorescent proteins for imaging neuronal activity. Nature. 2013:499.

Corty MM, Matthews BJ, Grueber WB. Molecules and mechanisms of dendrite development in Drosophila. Development. 2009; 136:1049–1061. [PubMed: 19270170]

Dacks AM, Green DS, Root CM, Nighorn AJ, Wang JW. Serotonin modulates olfactory processing in the antennal lobe of Drosophila. Journal of neurogenetics. 2009; 23:366–377. [PubMed: 19863268]

Dash PK, Hochner B, Kandel ER. Injection of the cAMP-responsive element into the nucleus of Aplysia sensory neurons blocks long-term facilitation. Nature. 1990; 345:718–721. [PubMed: 2141668]

Deeg KE, Aizenman CD. Sensory modality-specific homeostatic plasticity in the developing optic tectum. Nat Neurosci. 2011; 14:548–550. [PubMed: 21441922]

Fabre V, Boutrel B, Hanoun N, Lanfumey L, Fattaccini CM, Demeneix B, Adrien J, Hamon M, Martres MP. Homeostatic regulation of serotonergic function by the serotonin transporter as revealed by nonviral gene transfer. J Neurosci. 2000; 20:5065–5075. [PubMed: 10864964]

Fields H. State-dependent opioid control of pain. Nat Rev Neurosci. 2004; 5:565–575. [PubMed: 15208698]

Freedman R, Adler LE, Myles-Worsley M, Nagamoto HT, Miller C, Kisley M, McRae K, Cawthra E, Waldo M. Inhibitory gating of an evoked response to repeated auditory stimuli in schizophrenic and normal subjects. Human recordings, computer simulation, and an animal model. Arch Gen Psychiatry. 1996; 53:1114–1121. [PubMed: 8956677]

Gaudry Q, Kristan WB Jr. Behavioral choice by presynaptic inhibition of tactile sensory terminals. Nat Neurosci. 2009; 12:1450–1457. [PubMed: 19801989]

Glaser T, Traber J. Binding of the putative anxiolytic TVX Q 7821 to hippocampal 5-hydroxytryptamine (5-HT) recognition sites. Naunyn Schmiedebergs Arch Pharmacol. 1985; 329:211–215. [PubMed: 3160954]

Gordon MD, Scott K. Motor control in a Drosophila taste circuit. Neuron. 2009; 61:373–384. [PubMed: 19217375]

Gou B, Liu Y, Guntur AR, Stern U, Yang CH. Mechanosensitive neurons on the internal reproductive tract contribute to egg-laying-induced acetic acid attraction in Drosophila. Cell Rep. 2014; 9:522–530. [PubMed: 25373900]

Griffith LC, Budnik V. Plasticity and second messengers during synapse development. Int Rev Neurobiol. 2006; 75:237–265. [PubMed: 17137931]

Grueber WB, Ye B, Moore AW, Jan LY, Jan YN. Dendrites of distinct classes of Drosophila sensory neurons show different capacities for homotypic repulsion. Curr Biol. 2003; 13:618–626. [PubMed: 12699617]

Grueber WB, Ye B, Yang CH, Younger S, Borden K, Jan LY, Jan YN. Projections of Drosophila multidendritic neurons in the central nervous system: links with peripheral dendrite morphology. Development. 2007; 134:55–64. [PubMed: 17164414]

Hodge JJ. Ion channels to inactivate neurons in Drosophila. Frontiers in molecular neuroscience. 2009; 2:13. [PubMed: 19750193]

Honjo K, Hwang RY, Tracey WD Jr. Optogenetic manipulation of neural circuits and behavior in Drosophila larvae. Nat Protoc. 2012; 7:1470–1478. [PubMed: 22790083]

Hu A, Zhang W, Wang Z. Functional feedback from mushroom bodies to antennal lobes in the Drosophila olfactory pathway. Proceedings of the National Academy of Sciences of the United States of America. 2010; 107:10262–10267. [PubMed: 20479249]

Hubel DH, Wiesel TN. The period of susceptibility to the physiological effects of unilateral eye closure in kittens. The Journal of physiology. 1970; 206:419–436. [PubMed: 5498493]

Huser A, Rohwedder A, Apostolopoulou AA, Widmann A, Pfitzenmaier JE, Maiolo EM, Selcho M, Pauls D, von Essen A, Gupta T, et al. The serotonergic central nervous system of the Drosophila larva: anatomy and behavioral function. PLoS One. 2012; 7:e47518. [PubMed: 23082175]

Hwang RY, Zhong L, Xu Y, Johnson T, Zhang F, Deisseroth K, Tracey WD. Nociceptive neurons protect Drosophila larvae from parasitoid wasps. Curr Biol. 2007; 17:2105–2116. [PubMed: 18060782]

Iwasaki Y, Tanabe M, Kobata K, Watanabe T. TRPA1 agonists--allyl isothiocyanate and cinnamaldehyde--induce adrenaline secretion. Bioscience, biotechnology, and biochemistry. 2008; 72:2608–2614.

Johns DC, Marx R, Mains RE, O'Rourke B, Marban E. Inducible genetic suppression of neuronal excitability. J Neurosci. 1999; 19:1691–1697. [PubMed: 10024355]

Jovanic T, Schneider-Mizell CM, Shao M, Masson JB, Denisov G, Fetter RD, Mensh BD, Truman JW, Cardona A, Zlatic M. Competitive Disinhibition Mediates Behavioral Choice and Sequences in Drosophila. Cell. 2016; 167:858–870. e819. [PubMed: 27720450]

Kandel ER. The molecular biology of memory storage: a dialogue between genes and synapses. Science (New York, NY. 2001; 294:1030–1038.

Kim JH, Wang X, Coolon R, Ye B. Dscam expression levels determine presynaptic arbor sizes in Drosophila sensory neurons. Neuron. 2013; 78:827–838. [PubMed: 23764288]

Klapoetke NC, Murata Y, Kim SS, Pulver SR, Birdsey-Benson A, Cho YK, Morimoto TK, Chuong AS, Carpenter EJ, Tian Z, et al. Independent optical excitation of distinct neural populations. Nature methods. 2014; 11:338–346. [PubMed: 24509633]

Kuner R. Central mechanisms of pathological pain. Nature medicine. 2010; 16:1258–1266.

Lesch KP, Waider J. Serotonin in the modulation of neural plasticity and networks: implications for neurodevelopmental disorders. Neuron. 2012; 76:175–191. [PubMed: 23040814]

Lima SQ, Miesenbock G. Remote control of behavior through genetically targeted photostimulation of neurons. Cell. 2005; 121:141–152. [PubMed: 15820685]

Macleod GT, Marin L, Charlton MP, Atwood HL. Synaptic vesicles: test for a role in presynaptic calcium regulation. J Neurosci. 2004; 24:2496–2505. [PubMed: 15014125]

Macpherson LJ, Zaharieva EE, Kearney PJ, Alpert MH, Lin TY, Turan Z, Lee CH, Gallio M. Dynamic labelling of neural connections in multiple colours by trans-synaptic fluorescence complementation. Nature communications. 2015; 6:10024.

Maj J, Chojnacka-Wojcik E, Tatarczynska E, Klodzinska A. Central action of ipsapirone, a new anxiolytic drug, on serotoninergic, noradrenergic and dopaminergic functions. J Neural Transm. 1987; 70:1–17. [PubMed: 2889795]

Matsunaga T, Fushiki A, Nose A, Kohsaka H. Optogenetic perturbation of neural activity with laser illumination in semi-intact drosophila larvae in motion. J Vis Exp. 2013:e50513. [PubMed: 23851598]

McCormick DA, Bal T. Sensory gating mechanisms of the thalamus. Current opinion in neurobiology. 1994; 4:550–556. [PubMed: 7812144]

Menon KP, Carrillo RA, Zinn K. Development and plasticity of the Drosophila larval neuromuscular junction. Wiley Interdiscip Rev Dev Biol. 2013; 2:647–670. [PubMed: 24014452]

Nicolai LJ, Ramaekers A, Raemaekers T, Drozdzecki A, Mauss AS, Yan J, Landgraf M, Annaert W, Hassan BA. Genetically encoded dendritic marker sheds light on neuronal connectivity in Drosophila. Proceedings of the National Academy of Sciences of the United States of America. 2010; 107:20553–20558. [PubMed: 21059961]

Nitabach MN, Blau J, Holmes TC. Electrical silencing of Drosophila pacemaker neurons stops the free-running circadian clock. Cell. 2002; 109:485–495. [PubMed: 12086605]

Ohyama T, Schneider-Mizell CM, Fetter RD, Aleman JV, Franconville R, Rivera-Alba M, Mensh BD, Branson KM, Simpson JH, Truman JW, et al. A multilevel multimodal circuit enhances action selection in Drosophila. Nature. 2015; 520:633–639. [PubMed: 25896325]

Olsen SR, Wilson RI. Lateral presynaptic inhibition mediates gain control in an olfactory circuit. Nature. 2008; 452:956–960. [PubMed: 18344978]

Prieto-Godino LL, Diegelmann S, Bate M. Embryonic origin of olfactory circuitry in Drosophila: contact and activity-mediated interactions pattern connectivity in the antennal lobe. PLoS Biol. 2012; 10:e1001400. [PubMed: 23055825]

Raymond JR, Mukhin YV, Gettys TW, Garnovskaya MN. The recombinant 5-HT1A receptor: G protein coupling and signalling pathways. Br J Pharmacol. 1999; 127:1751–1764. [PubMed: 10482904]

Reiff DF, Ihring A, Guerrero G, Isacoff EY, Joesch M, Nakai J, Borst A. In vivo performance of genetically encoded indicators of neural activity in flies. J Neurosci. 2005; 25:4766–4778. [PubMed: 15888652]

Reiff DF, Thiel PR, Schuster CM. Differential regulation of active zone density during long-term strengthening of Drosophila neuromuscular junctions. J Neurosci. 2002; 22:9399–9409. [PubMed: 12417665]

Riad M, Garcia S, Watkins KC, Jodoin N, Doucet E, Langlois X, el Mestikawy S, Hamon M, Descarries L. Somatodendritic localization of 5-HT1A and preterminal axonal localization of 5-HT1B serotonin receptors in adult rat brain. The Journal of comparative neurology. 2000; 417:181–194. [PubMed: 10660896]

Robinson IM, Ranjan R, Schwarz TL. Synaptotagmins I and IV promote transmitter release independently of Ca(2+) binding in the C(2)A domain. Nature. 2002; 418:336–340. [PubMed: 12110845]

Root CM, Masuyama K, Green DS, Enell LE, Nassel DR, Lee CH, Wang JW. A presynaptic gain control mechanism fine-tunes olfactory behavior. Neuron. 2008; 59:311–321. [PubMed: 18667158]

Ruiz-Canada C, Budnik V. Synaptic cytoskeleton at the neuromuscular junction. Int Rev Neurobiol. 2006; 75:217–236. [PubMed: 17137930]

Salvaterra PM, Kitamoto T. Drosophila cholinergic neurons and processes visualized with Gal4/UAS-GFP. Brain Res Gene Expr Patterns. 2001; 1:73–82. [PubMed: 15018821]

Shafer OT, Kim DJ, Dunbar-Yaffe R, Nikolaev VO, Lohse MJ, Taghert PH. Widespread Receptivity to Neuropeptide PDF throughout the Neuronal Circadian Clock Network of Drosophila Revealed by Real-Time Cyclic AMP Imaging. Neuron. 2008; 58:223–237. [PubMed: 18439407]

Singh RS, Hickey DA, David J. Genetic Differentiation between Geographically Distant Populations of DROSOPHILA MELANOGASTER. Genetics. 1982; 101:235–256. [PubMed: 17246085]

Stewart BA, Atwood HL, Renger JJ, Wang J, Wu CF. Improved stability of Drosophila larval neuromuscular preparations in hemolymph-like physiological solutions. Journal of Comparative Physiology a-Sensory Neural and Behavioral Physiology. 1994:175.

Struhl G, Basler K. Organizing activity of wingless protein in Drosophila. Cell. 1993; 72:527–540. [PubMed: 8440019]

Sultana T, Savage GP, McNeil DL, Porter NG, Clark B. Comparison of flavour compounds in wasabi and horseradish. J Food Agric Environ. 2003; 1:117–121.

Traber J, Davies MA, Dompert WU, Glaser T, Schuurman T, Seidel PR. Brain serotonin receptors as a target for the putative anxiolytic TVX Q 7821. Brain Res Bull. 1984; 12:741–744. [PubMed: 6541079]

Vogelstein JT, Park Y, Ohyama T, Kerr RA, Truman JW, Priebe CE, Zlatic M. Discovery of brainwide neural-behavioral maps via multiscale unsupervised structure learning. Science (New York, NY. 2014; 344:386–392.

Wang X, Kim JH, Bazzi M, Robinson S, Collins CA, Ye B. Bimodal control of dendritic and axonal growth by the dual leucine zipper kinase pathway. PLoS Biol. 2013; 11:e1001572. [PubMed: 23750116]

Westenberg HG, Gerritsen TW, Meijer BA, van Praag HM. Kinetics of l-5-hydroxytryptophan in healthy subjects. Psychiatry Res. 1982; 7:373–385. [PubMed: 6187038]

Wu H, Zhang GA, Zeng S, Lin KC. Extraction of allyl isothiocyanate from horseradish (Armoracia rusticana) and its fumigant insecticidal activity on four stored-product pests of paddy. Pest Manag Sci. 2009; 65:1003–1008. [PubMed: 19459178]

Xiang Y, Yuan Q, Vogt N, Looger LL, Jan LY, Jan YN. Light-avoidance-mediating photoreceptors tile the Drosophila larval body wall. Nature. 2010; 468:921–926. [PubMed: 21068723]

Yang L, Li R, Kaneko T, Takle K, Morikawa RK, Essex L, Wang X, Zhou J, Emoto K, Xiang Y, et al. Trim9 regulates activity-dependent fine-scale topography in Drosophila. Curr Biol. 2014; 24:1024–1030. [PubMed: 24746793]

Yao ZP, Macara AM, Lelito KR, Minosyan TY, Shafer OT. Analysis of functional neuronal connectivity in the Drosophila brain. Journal of neurophysiology. 2012:108.

Yuan Q, Joiner WJ, Sehgal A. A sleep-promoting role for the Drosophila serotonin receptor 1A. Curr Biol. 2006; 16:1051–1062. [PubMed: 16753559]

Yuan Q, Xiang Y, Yan Z, Han C, Jan LY, Jan YN. Light-induced structural and functional plasticity in Drosophila larval visual system. Science (New York, NY). 2011; 333:1458–1462.

Zemelman BV, Lee GA, Ng M, Miesenbock G. Selective photostimulation of genetically chARGed neurons. Neuron. 2002; 33:15–22. [PubMed: 11779476]

Zhang Y. Allyl isothiocyanate as a cancer chemopreventive phytochemical. Mol Nutr Food Res. 2010; 54:127–135. [PubMed: 19960458]

Zhang Y, Lu H, Bargmann CI. Pathogenic bacteria induce aversive olfactory learning in Caenorhabditis elegans. Nature. 2005; 438:179–184. [PubMed: 16281027]

## HIGHLIGHTS

- Sensory experience alters the nociceptive circuit and behavior in *Drosophila*.
- The nociceptive-input-induced plasticity in larvae is sensory-pathway-specific.
- Nociceptors activate serotonergic interneurons via second-order neurons (SONs).
- Serotonergic signaling inhibits nociceptor-to-SON synaptic transmission.

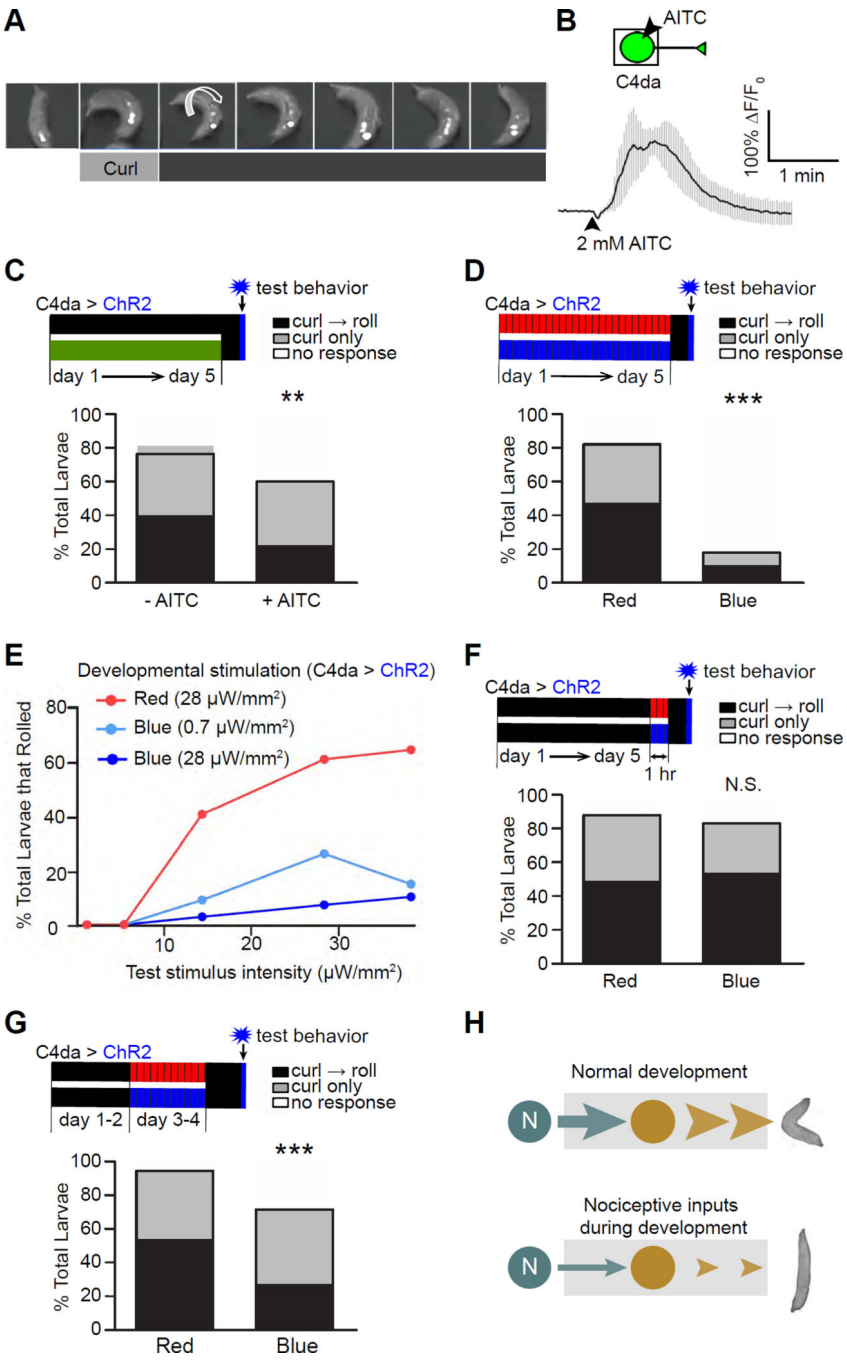


**Figure 1. Activation of larval nociceptors during development suppresses nociceptive behavior in mature larvae**

(**A**) A montage showing nociceptive behavior responses, including curling and rolling, in a 3rd instar larva. ChR2 was expressed specifically in C4da nociceptors and activated by illumination with blue light. Small arrows point to the openings of dorsal trachea to indicate the larva's body position, and the large arrow indicates the direction of rolling.

(**B**) AITC activates C4da neurons. The boxed area in the schematic indicates the part of the cell imaged for calcium signals. The trace shows the average of responses. $n = 3$. Error bars are SEM in all figures in this paper.

(**C**) Larvae raised on AITC exhibit reduced nociceptive behavior. Top panel: a diagram showing the experimental scheme. The developmental timeline of larvae is shown as days 1–5, with day 1 being the first day of development after egg laying (AEL) and day 5 being the time when the larvae are at the late 3$^{rd}$ instar stage. Control larvae were reared on regular food throughout development (black bar), whereas experimental larvae were reared on food containing 2.5 mM AITC (green bar). The vertical blue bar indicates the blue light used in optogenetic stimulation for behavioral tests on day 5, and the vertical black bar indicates the 1 hr of darkness prior to the tests. Throughout the paper, the following color coding is used: green for AITC; black for darkness or no AITC; red for red light (617 nm); blue for blue light (470 nm); and gray for ATP. Moreover, the expression of proteins for stimulating nociceptors (i.e., ChR2, CsChrimson, and $P2X_2$) is indicated by "C4da > proteins" above the timeline bars. $n = 75$ larvae per group. Bars represent the percentage of total larvae that performed rolling following curling ("curl → roll"), curling only, and no response. Note that every roll starts with curling.

(**D**) Optogenetic stimulation of nociceptors during larval development leads to a dramatic suppression of nociceptive behavior. $n = 45$ larvae per group.

(**E**) Developmental stimulation suppresses the maximal response of nociceptive behavior in mature larvae. Larvae that expressed ChR2 in C4da neurons were reared under pulses of red (28 μW/mm$^2$) or blue light (0.7 or 28 μW/mm$^2$) during development. Rolling responses of late 3$^{rd}$-instar larvae were tested with 5 different intensities of blue light (0.7, 5, 14, 28, and 38 μW/mm$^2$). $n = 115$, 88, and 69 larvae for red, 0.7 μW/mm$^2$ blue, and 28 μW/mm$^2$ blue, respectively.

(**F**) Larvae that received acute stimulation (1 hr) of nociceptors do not exhibit suppression of nociceptive behavior. $n = 60$ larvae per group.

(**G**) Stimulating nociceptors on days 3–4 AEL (early 3$^{rd}$ instar larval stage) suppressed nociceptive behavior in mature larvae tested on day 5 (i.e., 24 hrs after pulse stimulation). $n = 100$ larvae for each group.

(**H**) A set of diagrams that summarize the results in this figure. Stimulation of nociceptors during development leads to suppression of nociceptive behavior in mature larvae.

(See also Figures S1 and S2)

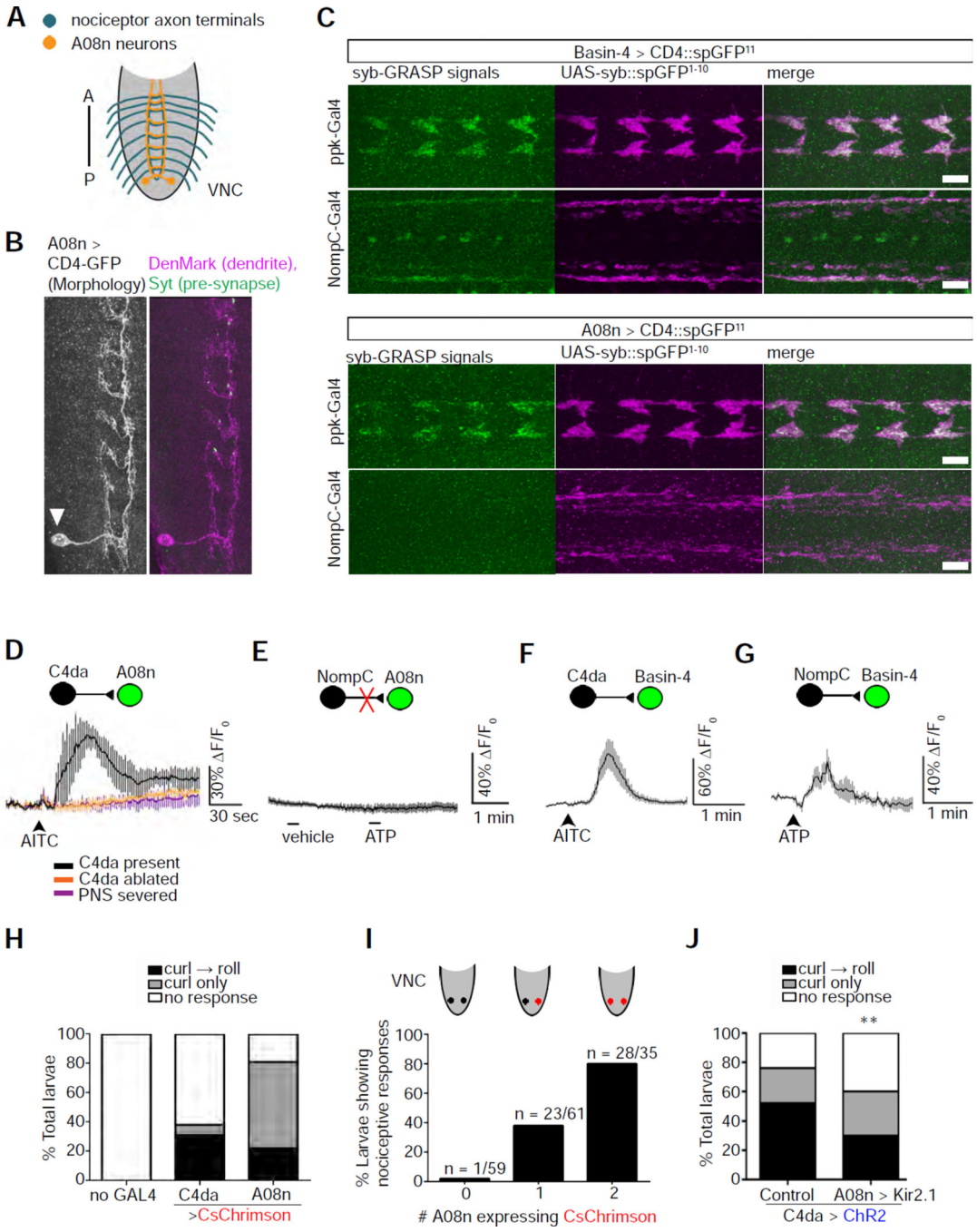


**Figure 2. A08n neurons are specific postsynaptic targets of nociceptors**

(**A**) A schematic of the axon projections of nociceptors (blue) and the neurites of A08n within the VNC (orange). A: anterior; P: posterior.

(**B**) The majority of A08n neurites are dendrites. A single A08n neuron labeled by the FLP-out technique. The soma (arrowhead) of the A08n neuron is located near the posterior end of the VNC. A08n neurites in close proximity to C4da axon terminals are mostly positive for the dendrite marker, DenMark, and contain scattered spots that are positive for the axonal marker, Synaptotagmin (Syt). Scale bar: 10 μm.

(**C**) A08n neurons are synaptic partners of C4da, but not NompC-expressing mechanosensory, neurons. The synaptobrevin (syb)-GRASP technique was used to detect synaptic connections between neurons. $SpGFP^{11}$ expressed in Basin-4 neurons produces syb-GRASP signals (green) with $spGFP^{1–10}$ (magenta) expressed in either nociceptors (*ppk*-GAL4) or mechanosensors (*NompC*-GAL4). In contrast, $spGFP^{11}$ expressed in A08n neurons only produces syb-GRASP signals with $spGFP^{1–10}$ in nociceptors. The discrete GFP signals along the VNC midline are artifacts that show up in the absence of $spGFP^{11}$ and can be observed with various antibodies. Scale bar: 10 μm.

(**D**) AITC activates A08n neurons specifically through C4da nociceptors, as shown by calcium imaging. A schematic is included to show pre- and post-synaptic neurons. The neuron that was recorded by GCaMP calcium imaging is shown in green. Traces show the averages of responses. No response was observed in the absence of C4da neurons (“C4da ablated”) or with the severing of nerves connecting the VNC with the PNS (“PNS severed”). $n$ = 3, 4, and 4 in “C4da present”, “C4da ablated”, and “PNS severed”, respectively.

(**E**) Stimulation of NompC-expressing mechanosensors does not activate A08n neurons. Mechanosensors expressing $P2X_2$ were stimulated by 1 mM ATP for $Ca^{2+}$ imaging. $n$ = 10 neurons (5 larvae).

(**F**) Stimulation of C4da nociceptors activates Basin-4 neurons. Note that AITC does not activate NompC-expressing mechanosensory neurons (data not shown). $n$ = 9 neurons (5 larvae).

(**G**) Stimulating NompC-expressing mechanosensors activates Basin-4 neurons. $n$ = 8 neurons (4 larvae).

(**H**) Activation of C4da or A08n neurons by CsChrimson elicits nociceptive response. $n$ = 90 larvae for each group. Note that activation of A08n neurons mostly results in abrupt body curling.

(**I**) Larvae expressing CsChrimson in one or two A08n neurons exhibit an increase in nociceptive behavior. Results combine curling and rolling. Most of the responders showed curling only. Sample numbers are indicated in the graph.

(**J**) Larvae with silenced A08n neurons show a significant reduction in nociceptive response. Nociceptors are activated by ChR2. A08n neurons were silenced by Kir2.1 expression with the GMR82E12-Gal4 driver. The control group lacks the driver. $n$ = 100 larvae for each group.

(See also Figure S3.)

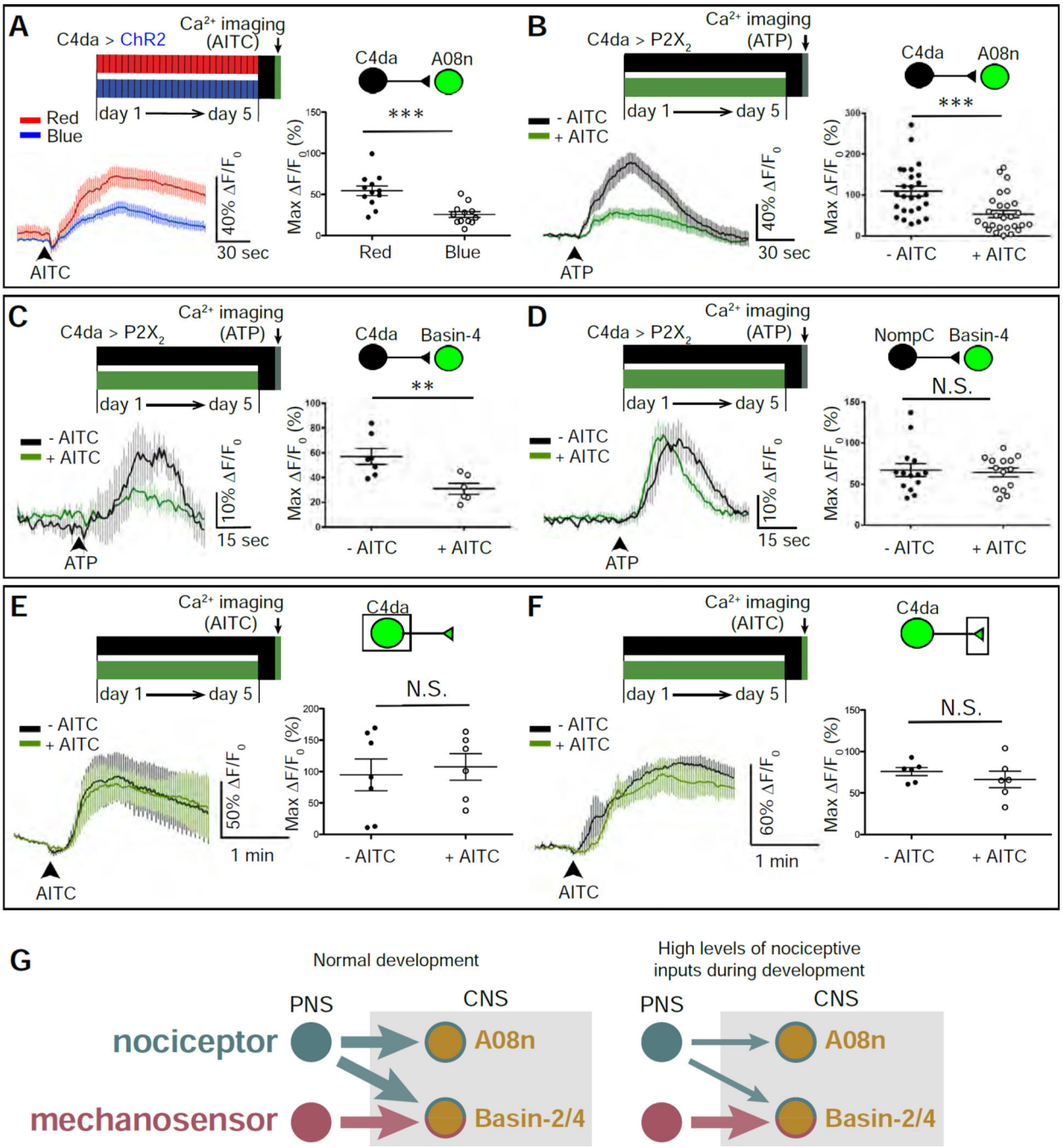


**Figure 3. The sensory-input-induced plasticity of larval nociceptive circuit is pathway-specific**

(**A**) Optogenetic activation of C4da neurons during development inhibits C4da-to-A08n transmission. C4da neurons in mature larvae were stimulated by AITC for $Ca^{2+}$ imaging. Max $\Delta F/F_0$ for individual A08n neurons are plotted on the graph and used for statistical analyses (i.e., each dot indicates one A08n). $n = 12$ neurons (from 6 larvae) per group. (**B**) Stimulation of C4da neurons by AITC (5 mM) during development inhibits C4da-to-A08n transmission. C4da neurons in mature larvae were stimulated by $P2X_2$ for $Ca^{2+}$

imaging. *n* =26 (from 13 larvae) and 28 neurons (from 14 larvae) in "-AITC" and "+AITC", respectively.

(**C**) Stimulation of C4da neurons by AITC (2.5 mM) during development inhibits C4da-to-Basin4 transmission. Because the responses of Basin-4 neurons are highly variable within each VNC (data not shown) (Jovanic et al., 2016), the average of Max $\Delta F/F_0$ of 10 Basin-4 neurons from abdominal segments 3 to 7 in each VNC were calculated to represent Basin-4 activity in each VNC (i.e., each dot indicates one larva). *n* = 7 and 6 larvae in "- AITC" and "+ AITC", respectively.

(**D**) Treating larvae with AITC (2.5 mM) during development does not alter the mechanosensor-to-Basin4 transmission. *n* = 14 larvae per group.

(**E–F**) Larvae raised in environments with and without AITC (2.5 mM) have similar levels of noxious stimulation-induced calcium responses in C4da somas (**E**) and axon terminals (**F**). (**E**) *n* = 6 and 7 neurons (4 larvae per group) in "- AITC" and "+ AITC", respectively. (**F**) *n* = 6 neurons from 3 larvae per group.

(**G**) Schematics showing the pathway-specificity of nociceptor-input-induced plasticity in synaptic connections between larval nociceptive and SONs in the circuit. Left: Circuit diagram of connections under normal developmental conditions. Right: High levels of nociceptive input specifically suppresses synaptic transmission from nociceptors to SONs. (See also Figure S4.)

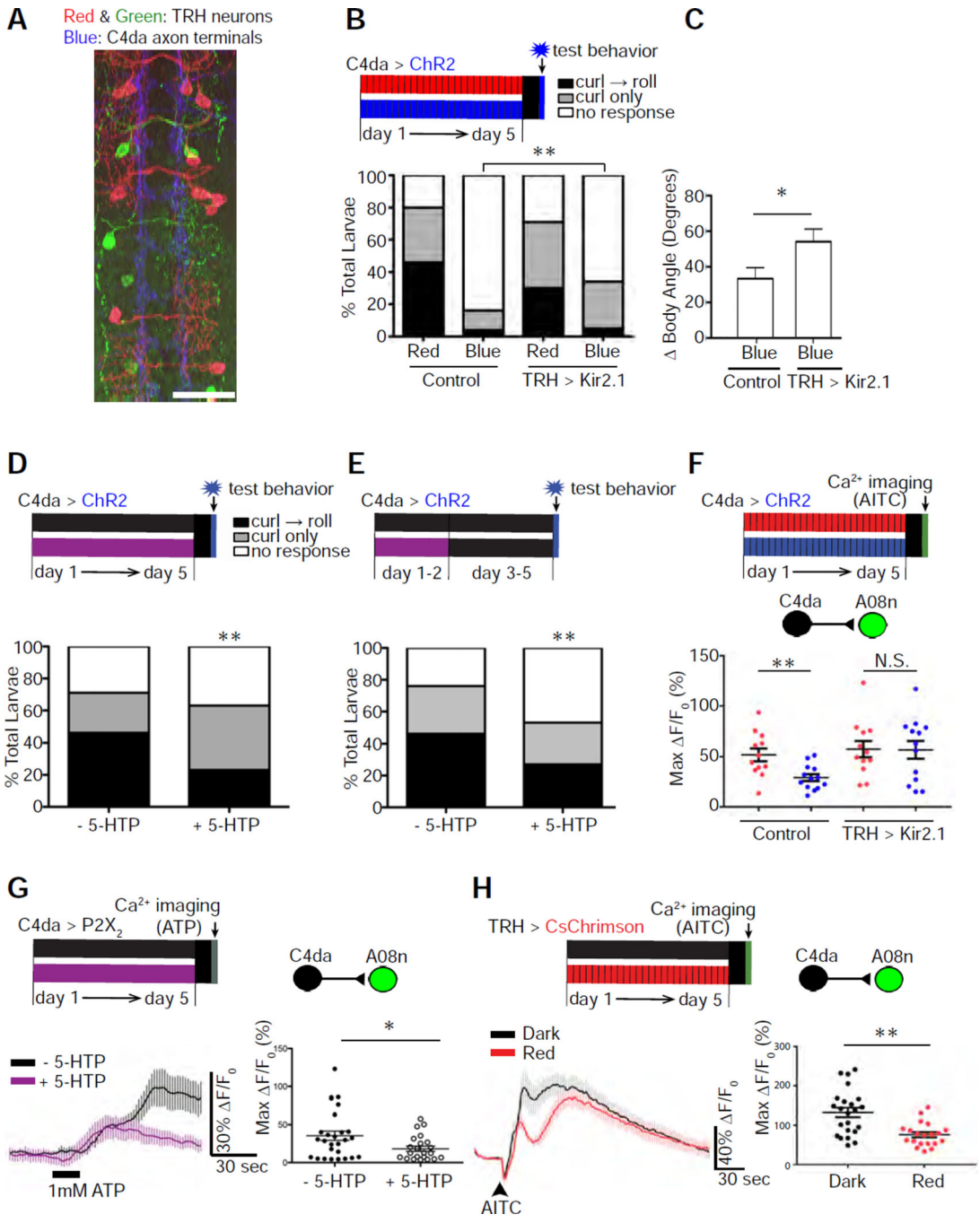


**Figure 4. Serotonergic neurons are required to establish sensory-input-induced plasticity of larval nociceptive behavior**

(**A**) Projections of serotonergic neurons overlap with C4da axon terminals. Serotonergic neurons (TRH), which were labeled by a multicolor FLP-out technique, are shown in red and green, and C4da axon terminals in blue. Scale bar: 25 μm.

(**B** & **C**) Silencing TRH neurons partially rescued nociceptive behavioral responses in larvae whose nociceptors were optogenetically stimulated during development. TRH neurons were silenced by Kir2.1 expression with TRH-Gal4. The control lacked TRH-Gal4. In (**B**), *n* =

120 (Control + Red), 120 (Control + Blue), 135 (TRH>Kir2.1 + Red), and 120 (TRH>Kir2.1 + Blue) larvae. In (**C**), *n* = 42 (TRH) and 40 (TRH>Kir.21) larvae.
(**D**) Larvae fed 5-HTP throughout development show a 2-fold reduction in rolling (**a**). *n* = 135 (−5-HTP) and 105 (+ 5-HTP) larvae.
(**E**) Larvae fed 5-HTP during days 1–2 of larval development show a 2-fold reduction in nociceptive rolling compared to control. *n* = 50 (− 5-HTP) and 60 (+ 5-HTP) larvae.
(**F**) Silencing TRH neurons rescues A08n activity in larvae that experience high levels of nociceptive inputs during development. Control: larvae that have normal TRH activity due to the lack of *TRH*-Gal4 driver for expressing UAS-Kir2.1 (*n* = 12 and 13, respectively, for red and blue illuminations). TRH>Kir2.1: larvae whose TRH neurons were silenced by the expression of Kir2.1 (*n* = 12 and 13, respectively, for red and blue illuminations).
(**G**) Larvae fed 5-HTP throughout development show a reduction in C4da-to-A08n synaptic transmission. *n* = 27 (− 5-HTP) and 23 (+ 5-HTP) neurons.
(**H**) Optogenetic stimulation of serotonergic neurons during development, without the stimulation during calcium imaging in mature larvae, reduced AITC-elicited A08n responses. Pulses of red light were used to chronically stimulate CsChrimson-expressing serotonergic neurons. Larvae in the control group were reared in the dark. *n* = 23 neurons (from 13 larvae) and 20 neurons (from 11 larvae) in dark and red, respectively.
(See also Figure S5.)

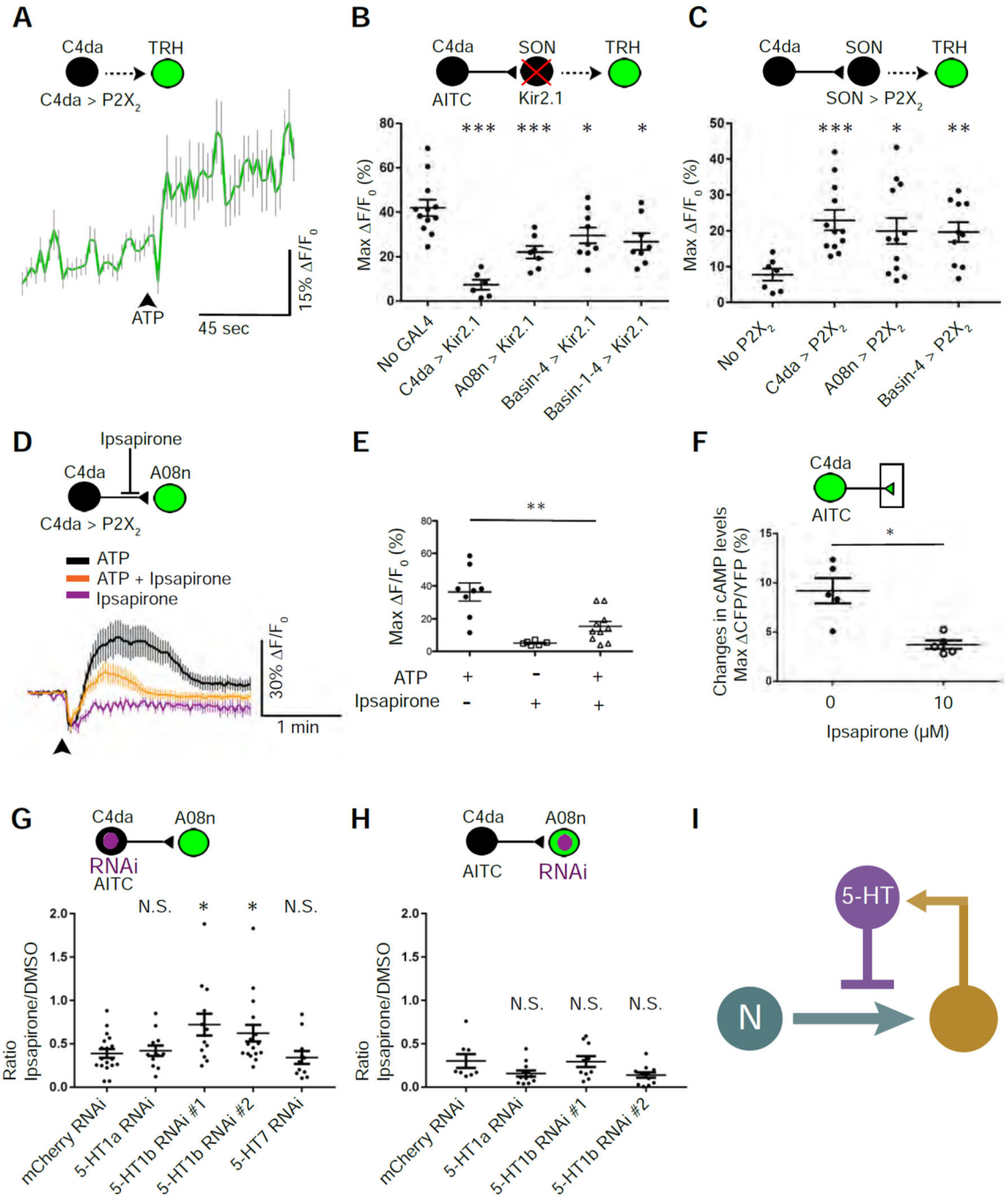


**Figure 5. Feedback inhibition of nociceptor-to-SON transmission through serotoninergic neurons**

(**A**) Stimulating C4da nociceptors activates serotonergic neurons. The trace shows the averages of GCaMP6f intensities in TRH neurons caused by stimulating C4da neurons via ATP/P2X$_2$. The black arrowhead indicates the start of ATP/P2X$_2$-mediated stimulation. $n$ = 33.

(**B**) Silencing SONs suppresses nociceptor-induced activation of serotonergic neurons. C4da, A08n, Basin-4, and Basin-1–4 were inhibited by expressing Kir2.1. AITC was used to

stimulate C4da neurons. *n* = 12, 6, 7, 9, and 8 larvae in control, C4da, A08n, Basin-4, and Basin-1–4 groups, respectively.

(**C**) Stimulation of SONs activates serotonergic neurons. ATP was used to activate neurons expressing $P2X_2$. Larvae in "No $P2X_2$" group had no $P2X_2$ expression due to the lack of a GAL4 driver and a $P2X_2$ transgene. *n* = 7, 12, 12, and 10 larvae in control, C4da, A08n, and Basin-4 groups, respectively.

(**D** & **E**) Ipsapirone (100 μM) inhibits C4da-to-A08n synaptic transmission. ATP/$P2X_2$ was used to activate C4da neurons. (**D**) Traces show the averages of responses. (**E**) Quantification and statistical analysis (*n* = 8, 6, 10 neurons, 5 larvae per group).

(**F**) Ipsapirone (10 μM) diminishes AITC-elicited increase in cAMP levels in C4da axon terminals. Imaging-based cAMP sensor, Epac1-camps, was expressed specifically in nociceptors, and their presynaptic terminals were imaged for Förster resonance energy transfer (FRET). AITC was used to activate nociceptors. Levels of cAMP were quantified as changes in the inverse FRET ratio, which is CFP intensity divided by YFP intensity (ΔCFP/YFP) scanned with a 458-nm confocal laser. *n* = 5 larvae per group.

(**G** & **H**) Knockdown of 5-HT1b in C4da neurons, but not that in A08n, significantly blocks the effect of ipsapirone on nociceptor-to-SON transmission. The graphs show the ratio of AITC-elicited Max $\Delta F/F_0$ in the presence of 10 μM ipsapirone over that in the presence of DMSO (vehicle). This ratio indicates the extent of serotonergic inhibition of AITC-elicited responses in A08n. In the schematic, neurons expressing GCaMP6f and RNAi are shown in green and purple, respectively. An RNAi line against mCherry was used as a negative control. 5-HT1b #1 (B-33418) and 5-HT1b #2 (B-27635) were used to knock down 5-HT1b. (**G**) *n* = 18 neurons (9 larvae), 12 neurons (6 larvae), 13 neurons (7 larvae), 17 neurons (9 larvae), and 12 neurons (7 larvae) for mCherry, 5-HT1a, 5-HT1b #1, 5-HT1b #2, and 5-HT7, respectively. (**H**) *n* = 8 (5 larvae), 12 (6 larvae), 10 neurons (5 larvae), and 12 neurons (6 larvae) for mCherry, 5-HT1a, 5-HT1b #1, and 5-HT1b #2, respectively.

(**I**) Schematic model showing that serotonergic neurons modulate nociceptor-to-SON transmission by providing feedback inhibition.

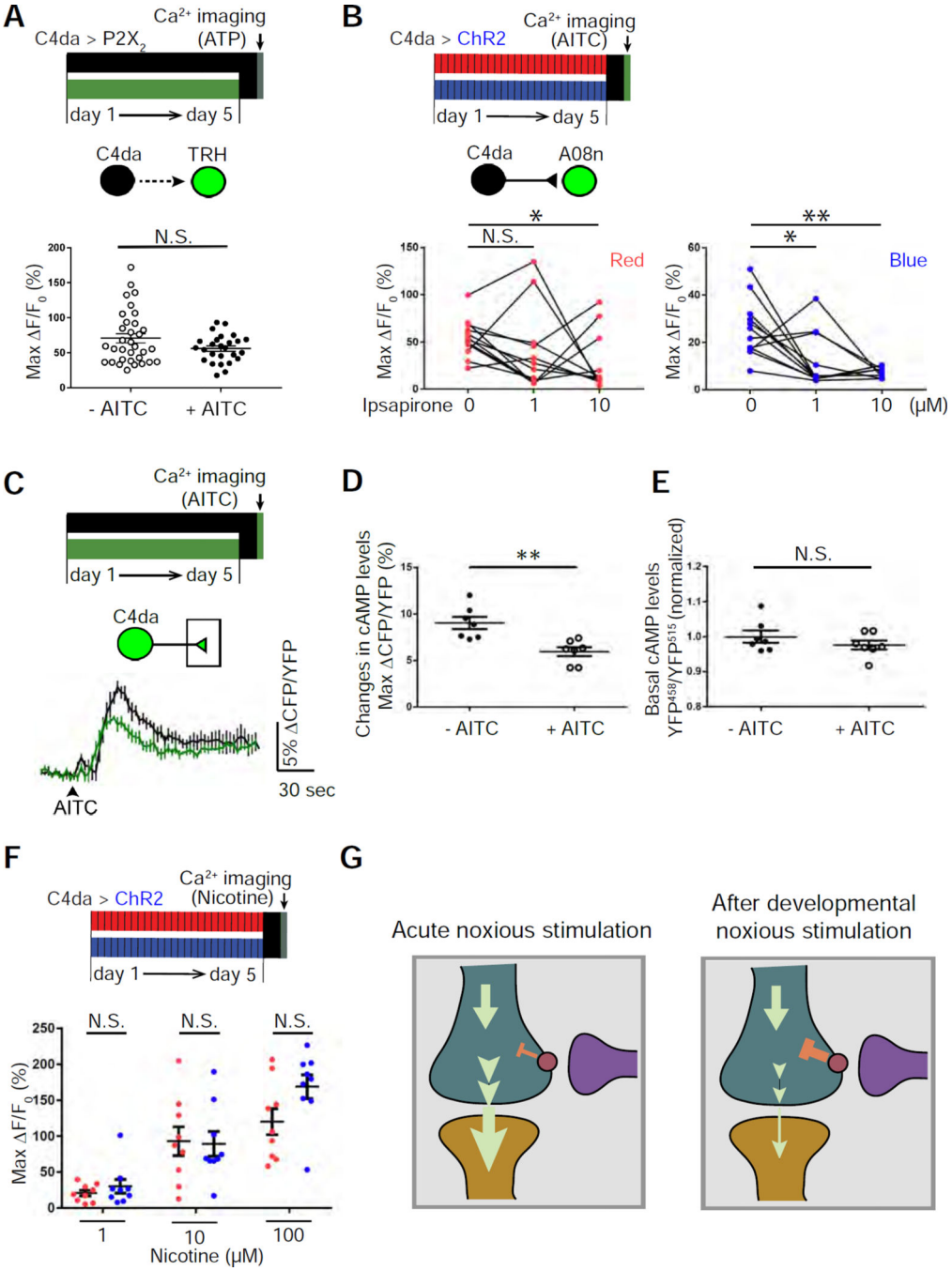


**Figure 6. Developmental stimulation of nociceptors enhances 5-HT receptor-mediated inhibition of nociceptor-to-target transmission**

(**A**) Noxious stimulation during development (2.5 mM AITC) does not affect nociceptor-induced responses in serotonergic neurons. *n* = 33 and 25 larvae for "- AITC" and "+ AITC", respectively.

(**B**) Developmental stimulation of C4da neurons sensitizes C4da-to-A08n transmission to ipsapirone. AITC was used to stimulate C4da neurons for calcium imaging. 0, 1, or 10 μM

ipsapirone was mixed with AITC and applied sequentially from low to high concentrations. $n$ = 12 neurons (from 6 larvae) for each group.

(**C–E**) Noxious stimulation during development (2.5 mM AITC) significantly diminishes AITC-elicited increase in cAMP levels in C4da axon terminals without affecting basal cAMP levels. (**C**) Average traces of cAMP responses. (**D**) Quantification and statistical analysis of cAMP levels. $n$ = 7 for each group. (**E**) Quantification and statistical analysis of basal cAMP levels. The value, $YFP^{458}/YFP^{515}$, was normalized by dividing the average of the "- AITC" group. $n$ = 7 for each group.

(**F**) Developmental activation of nociceptors does not reduce A08n responses to nicotine. Three different concentrations of nicotine were applied to the brains of mature larvae, and changes in calcium levels in A08n somata were analyzed. Since A08n is specific to nociceptive inputs, A08n responses to nicotine reflect its responses to nociceptive inputs. $n$ = 9 in each group.

(**G**) A model that explains the experience-dependent sensory-input-induced plasticity in nociceptor-to-SON transmission. Left panel: Acute noxious stimulation in mature larvae increases cAMP levels in the presynaptic terminals of nociceptors (shown in teal) and leads to robust synaptic transmission to SONs (shown in orange). Serotonergic neurons (shown in purple) suppress cAMP levels in nociceptor presynaptic terminals. Right panel: Developmental noxious stimulation enhances the responsiveness of nociceptor presynaptic terminals to 5-HT modulation in mature larvae, leading to further suppression of cAMP production and reduced synaptic transmission to target neurons.

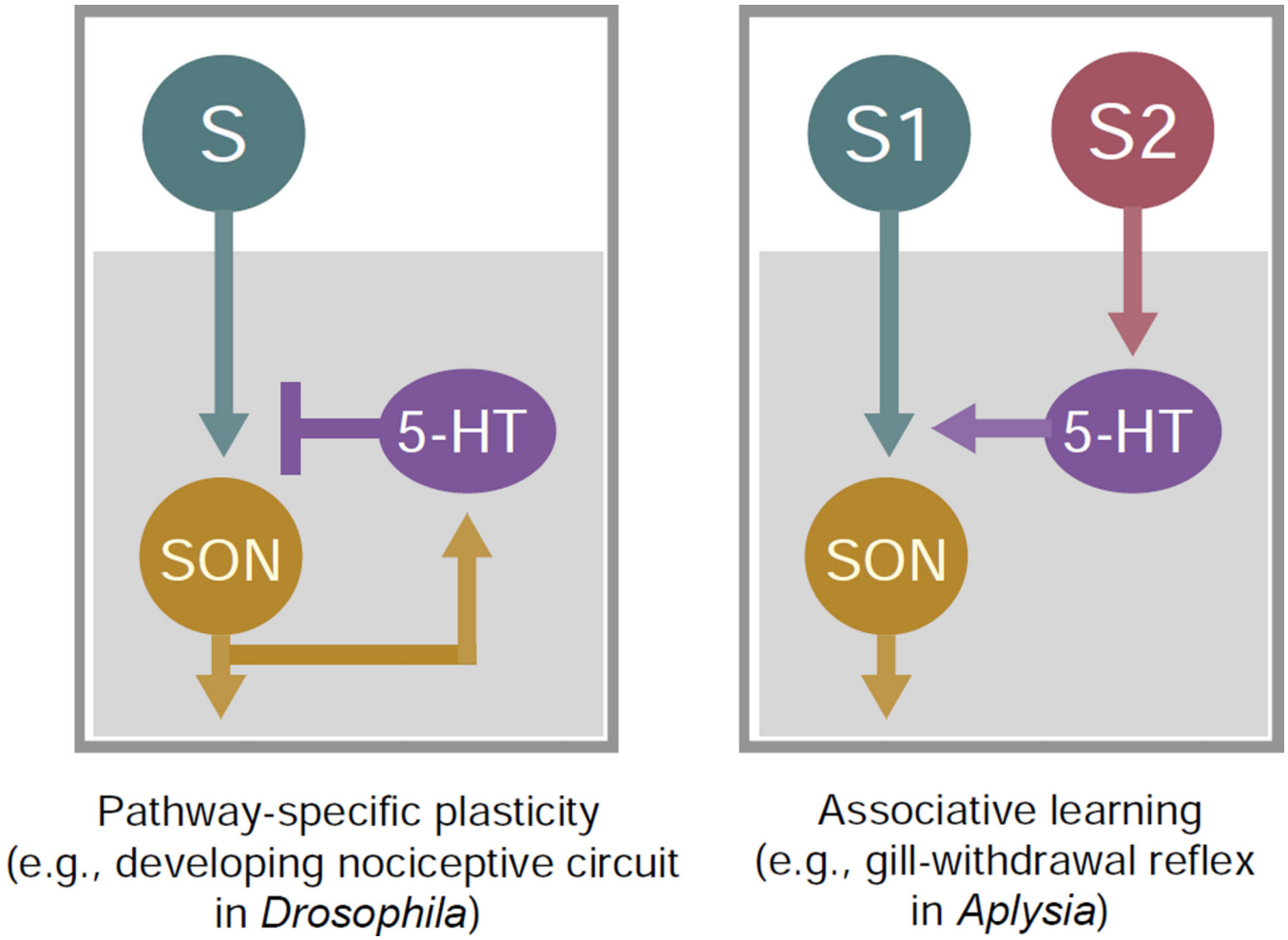


**Figure 7. Feedback modulation enables pathway-specific plasticity in developing sensory circuits in *Drosophila***

The pathway-specific plasticity of the developing nociceptive circuit in *Drosophila* is different from the serotonergic facilitation that occurs during sensitization of the defensive gill-withdrawal reflex in *Aplysia*. In the *Drosophila* nociceptive circuit, activity in nociceptors ("S") leads to activation of both SONs in the circuit and serotonergic interneurons ("5-HT"), while in *Aplysia* gill-withdrawal reflex circuit, serotonergic interneurons are activated by another sensory pathway (S2).